# A CHARGED RESIDUE IN THE TURRET OR OUTER PORE MOUTH OF hKv1.5 ALTERS MACROSCOPIC CURRENT KINETICS

by

LOGAN ERIC ELMER LEE

B.Sc. (Hons.), The University of British Columbia, 2003

A THESIS SUBMITTED IN PARTIAL FULFILLMENT OF THE REQUIREMENTS FOR THE DEGREE OF

MASTER OF SCIENCE

in

THE FACULTY OF GRADUATE STUDIES

PHYSIOLOGY

THE UNIVERSITY OF BRITISH COLUMBIA

August 2005

**Abstract**

Using hKv1.5 expressed in HEK-293 cells the roles of R487 and H463 in the processes of permeation and inactivation were studied. Mutation of the arginine at position 487 to a valine (R487V) alters the *I-V* relationship through Kv1.5 such that the normalized current at positive voltages, in symmetrical 140 mM $K^+$, is less than at negative voltages. The magnitude of current reduction at positive voltages was unaffected by extracellular acidification suggesting that the protonation state of H463 does not effect the rate of $K^+$ exit or entry at the outer pore mouth. Using an Eyring-rate model we have ascertained that the reduction in the normalized outward currents through R487V occurs through a change at the outer pore mouth that alters the permeation process. In addition to the role of R487V in the process of permeation, it has also been shown that a histidine residue at position 463 in Kv1.5 confers sensitivity to external protons and affects the rate of inactivation. To further investigate the role these residues, R487 and H463, on Kv1.5 macroscopic current kinetics we engineered a double mutant that swapped the residues at positions 463 and 487. In Kv1.5 H463R/R487H there was a decrease in the time constant for inactivation and an increase in the time constant for recovery from inactivation. Elevation of $K^+_o$ (140 mM) increased the time constant for inactivation and deactivation through a 'foot-in-the-door' mechanism by which elevated $K^+_o$ occupies an outer and inner binding site, respectively, at the selectivity filter and prevents the pore from collapsing. These results support the hypothesis that processes of activation/deactivation and inactivation are not separate entities, but rather, alterations of one parameter can have dramatic effects on the other in Kv1.5.

**Table of Contents**

**List of Figures**

## List of Symbols and Abbreviations

α: alpha
~: approximately
°: Degree
μ: micro ($10^{-6}$)
Ω: Ohm
τ: tau
A: Alanine
AChR: Acetylcholine Receptor
act: Activation
BK: Calcium-activated large conductance $K^+$ channel
C: Celsius
$Ca^{2+}$: Calcium ion
CFTR: Cystic fibrosis transmembrane conductance regulator
Cl: Chloride
$CO_2$: Carbon dioxide
$Cs^+$: Cesium ion
D: Aspartate
deact: Deactivation
DNA: Deoxyribonucleic acid
E: Glutamate
$E_{rev}$: Reversal potential
G: Glycine
g: Conductance
H: Histidine
$H^+$: Proton
HEPES: (N-[2-hydroxyethyl] piperazine-N'-[2-ethanesulfonic acid])
HEK: Human embryonic kidney
Hz: Hertz
I: Current
i: Inside
inact: Inactivation
K: Lysine
*k*: Slope factor
$K^+$: potassium ion
KcsA: *Streptomyces lividans* $K^+$ channel
Kv: Voltage-gated potassium channel
l: Litre
LM: Mouse tumor cell line
M: Molar
mV: Millivolt
ms: Millisecond
$g_{max}$: Maximal conductance
MEM: Minimal essential medium
MES: (2-[N-Morpholino] ethanesulfonic acid)

$Mg^{2+}$: Magnesium ion
min: Minute
MthK: *Methanobacterium thermoautotrophicum* $K^+$ channel
nA: Nanoampere
$Na^+$: Sodium ion
$Na_v$: Voltage-gated $Na^+$ channel
NMG: N-methyl-D-glucamine
o: Outside
P: Proline
p: pico ($10^{-15}$)
$P_K$: Permeability of $K^+$
$pK_H$: $-\log_{10}$ of the dissociation constant for half-protonation of a histidine residue
$P_{Na}$: Permeability of a Sodium ion
Q: Glutamine
R: Arginine
*R*: Gas Constant (8.314 KJ/mol/K)
$Rb^+$: Rubidium ion
S: Siemen
s: Second
Shaker-IR: Shaker channel with N-type inactivation removed
T: Threonine
*T*: Temperature
TAPS: (N-tris [Hydroxymethyl] methyl-3-amino-propanesulfonic acid
$TEA^+$: Tetraethylammonium
TM: Transmembrane segment
V: Valine
*V*: Voltage
$V_{1/2}$: Half-activation voltage
$V_H$: Holding potential
$V_m$: Membrane voltage
X: A non-conserved amino acid
Y: Tyrosine

**Acknowledgements**

I would like to thank my supervisor Dr. Steve Kehl for providing me the opportunity to work in his lab and his constant encouragement throughout my post-graduate education. I would like to thank Cyrus Eduljee for generating the Kv1.5 H463R/R487H and Kv1.5 H463Q/R487H mutants. I would like to acknowledge David Chiang and Daniel Kwan for making some of the solutions. Thanks to Dr. David Steele and Grace Wu for their assistance in learning the technique of site-directed mutagenesis and other molecular biology approaches. Thanks to Fifi Chiu and Yan Liu for preparing the cells and my supervisory committee, Dr. David Fedida and Dr. David Mathers, for their assistance in the preparation and submission of my thesis.

I would like to thank the Natural Sciences and Engineering Research Council of Canada for providing me a PGS-M scholarship.

## Introduction

### Structural Arrangement

Voltage gated potassium (Kv) channels are membrane proteins that are important in regulating the flow of potassium ions ($K^+$) across the membrane of all living cells (Hille 2001). In 1952, seminal experiments by Hodgkin and Huxley demonstrated the role of Kv channels during repolarization of an action potential in the squid giant axon (Hodgkin & Huxley, 1952b). Since the first description of voltage-gated ion channels there has been extensive research to determine the kinetics and gating of these channels (Hodgkin *et al.*, 1952; Hodgkin & Huxley, 1952b). Kv channels are comprised of 4 α-subunits with each subunit containing 6 transmembrane regions (S1-S6) (Tempel *et al.*, 1987; Kamb *et al.*, 1988; Mackinnon, 1991a; Mackinnon, 1991b). The 4 subunits, when viewed from the top, are arranged in a four-fold symmetry with a portion of each subunit (S5-P-S6) contributing to the formation of the pore (the permeation pathway) (Doyle *et al.*, 1998). The S1, S2, and S3 regions of the channel were originally hypothesized to form the outer most aspect of the channel, while the S4 segment is positioned at the center of the subunit, when viewed from above, and accounts for the voltage-sensing component (Hille 2001).

### Crystal Structure

X-ray crystallography of a $K^+$ channel from *Streptomyces lividans* (KcsA ) provided the first picture of the structure of $K^+$ channels. The KcsA $K^+$ channel is comprised of 4 α-subunits that have 2 transmembrane (TM) segments and a pore loop. The first TM segment, analogous to S5 in mammalian Kv channels, crosses the membrane from the cytoplasm to the extracellular space and constitutes the outer helix.

The sequence continues from the outer helix into the extracellular space as a short loop, the "turret", and then re-enters the membrane as the pore helix (Doyle *et al.*, 1998; Hille B, 2001) Within the pore helix of a $K^+$ channel lies 4 high affinity $K^+$ binding sites (Heginbotham *et al.*, 1994; Doyle *et al.*, 1998; Zhou *et al.*, 2001; Jiang *et al.*, 2002). The outer vestibule is a portion of the channel that lies above the selectivity filter and acts to concentrate cations and repel anions from the outer "mouth" of the pore; while the inner vestibule, ~10 angstroms wide, is positioned below the selectivity filter (Doyle *et al.*, 1998). The pore loop continues into TM2 and crosses the membrane from the outside to the inside of the channel as the inner helix (Doyle *et al.*, 1998).

**Ion Permeation**

The fundamental role of ion channels is to conduct ions, usually with some degree of selectivity, across a membrane. In Kv channels, membrane depolarization results in a conformational change of the S4 segment that opens the channel and allows $K^+$ ions to be preferentially conducted across the cell membrane (Elinder *et al.*, 2001). This selectivity of $K^+$ channels is surprising considering the small difference in the atomic radii of $Na^+$ and $K^+$, 0.95 angstroms and 1.33 angstroms, respectively (Mackinnon, 2003). Despite the difference in the atomic radii of $K^+$ and $Na^+$ ions, $K^+$ channels have a ~100-fold higher permeability ratio for $K^+$ ions over $Na^+$ ions ($P_{Na}:P_K = 0.01$) (Mackinnon, 2003).

$K^+$ channel selectivity occurs at a 'signature sequence (TXGYG) near the extracellular portion of the ion conducting pore (Heginbotham *et al.*, 1994). These residues are conserved in almost all $K^+$-selective channels confirming the importance of this sequence. Mutational analysis has shown that alterations of this sequence result in a significantly reduced selectivity, or a complete loss of ion conduction (Heginbotham *et*

*al.*, 1994). Within the selectivity filter of Kv channels there are 4-evenly spaced binding sites, formed by carbonyl oxygen and hydroxyl oxygen groups of threonine residues, which stabilize $K^+$ ions in the permeation pathway. The partially negative charge of the hydroxyl or carbonyl oxygen (similar to the negative charge on the oxygen atom of a water molecule) reduces the energetic cost for a dehydrated $K^+$ ion to permeate the pore, and stabilizes $K^+$ ions at their binding sites within the pore.

As previously stated, there are 4 $K^+$ ions binding sites in Kv channels (Zhou *et al.*, 2001). The occupancy of these sites is structured such that no 2 adjacent sites are ever occupied, and ions move through the pore in either a 1,3 or 2,4 conformation (Figure 1B) (Zhou *et al.*, 2001). It is thought that the movement of ions through the permeation pathway is not coupled but somewhat dependent (in that no 2 adjacent sites can be occupied), on the flux of other ions from their binding sites. For example, in the KcsA $K^+$ channel permeation cycle, for the pore to go from a 2,4 to a 1,3 configuration, the internal binding site (site 4) must first be vacated. After this ion leaves the pathway, the $K^+$ ion at position 2 can move to the 3$^{rd}$ site, and a new $K^+$ ion can enter the permeation pathway to bind at position 1 (Figure 1B).

The flux of $K^+$ across the cell membrane is partially regulated by the concentration of the ionic species on either side of the pore. A reduction of $K^+_i$ decreases the occupancy of the pore and causes a conformational change (G77 pinches the permeation pathway shut in KcsA) at the selectivity filter that increases the affinity of the external binding site for $K^+$ (Zhou *et al.*, 2001). The change in the affinity of the binding sites increases the dwell time for $K^+$ ions in the pore and decreases the rate at which $K^+$ is able to leave the pore (Mackinnon, 2003).

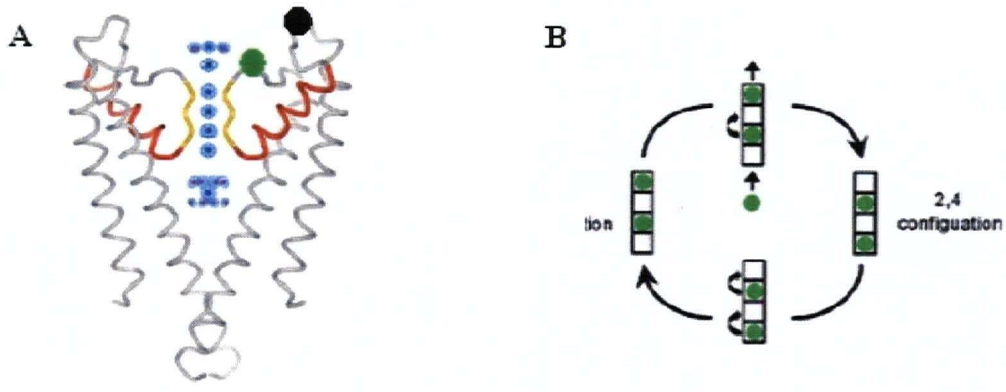


(Mackinnon, 2003)

Figure 1 **The permeation pathway of Kv channels. A**, A side view of 2 α-subunits of the KcsA $K^+$ channel with the extracellular surface on the top. The subunits in the front and back of the channel have been removed to view the permeation pathway of the channel. Each subunit contributes to the selectivity filter (gold), the pore (red) and the outer and inner vestibules. The green and black circles in Figure 1A represent the approximate positions of R487 of H463, respectively, in Kv1.5. **B**, A permeation cycle for $K^+$ ion flux in Kv channels is adopted by having a 1.3, or 2,4 configuration for $K^+$ ions binding within the pore. For the permeation cycle to go from a 2,4 to 1,3 pore configuration, the $K^+$ ion at the position adjacent to the intracellular solution (site 4) must exit the permeation pathway and enter the bulk solution. With site 4 vacant, the $K^+$ ion at position 2 can go to the 3rd binding site. A $K^+$ ion is now able to enter the permeation pathway, from the extracellular solution, and bind to the 1st binding site. Vacant binding sites are occupied by water molecules.

**Charges in the Inner and Outer Vestibule Regulate Ion Permeation**

The single channel conductance of $K^+$ channels is generally on the order of 5-50 pS, however, $Ca^{2+}$ activated potassium (BK) channels have a single channel conductance of ~300 pS, roughly 6-fold larger than most Kv channels (Latorre, 1989; Latorre *et al.*, 1989). Mutational analysis in KcsA (Nimigean *et al.*, 2003), a *Methanobacterium thermoautotrophicum* $K^+$ channel (MthK) (Nimigean *et al.*, 2003; Brelidze *et al.*, 2003), a Cystic fibrosis transmembrane conductance regulator (CFTR) (Smith *et al.*, 2001), $Na_v$ (Li *et al.*, 2000), Kv2.1 (Consiglio *et al.*, 2003), and BK (Nimigean *et al.*, 2003; Brelidze *et al.*, 2003) channels have demonstrated that charged residues act to concentrate ions at the inner and outer vestibules increasing their 'effective' concentration.

## Activation Gating

### S4 as the primary voltage sensor

From studies performed on the squid giant axon it has been shown that there is a high degree of voltage sensitivity to the opening of potassium and sodium channels (Hodgkin *et al.*, 1952; Hodgkin & Huxley, 1952a; Hodgkin & Huxley, 1952b). From the results in these studies, which investigated the kinetic properties of $Na_v$ and Kv channels, it was suggested that Kv and $Na_v$ channels open through a displacement of charge with depolarization. The delay in channel opening (activation) suggests that this process occurs through a multiple step sequence.

In *Shaker* Kv channels it has been shown that during activation the total gating charge per channel is ~$13e_0$ (Hoshi *et al.*, 1994; Zagotta *et al.*, 1994b; Aggarwal & Mackinnon, 1996; Seoh *et al.*, 1996) and that the first charge movement associated with depolarization is less voltage dependent (Sigg *et al.*, 1994; Perozo *et al.*, 1994). It has since been shown that charge mobilization in *Shaker* channels is a multiple step process and that there are five transitions between the closed and open state (Hoshi *et al.*, 1994; Zagotta *et al.*, 1994b). It was determined in *Shaker* that a single open state existed because the distribution of open times fit a single exponential function (Hoshi *et al.*, 1994).

The mechanism of voltage sensing is thought to be primarily by the S4 TM segment in Kv channels. In the S4 segment of Kv channels it has been shown that approximately every third amino acid is a positively charged residue (K or R) (Aggarwal & Mackinnon, 1996; Larsson *et al.*, 1996; Yang *et al.*, 1996). This topology is highly conserved in voltage-gated channels. Several studies in *Shaker* channels have shown that

mutation of these residues (to negatively or neutrally charged residues) results in ablation or alteration of the voltage sensing mechanism (Liman *et al.*, 1991; Bezanilla *et al.*, 1991; Papazian *et al.*, 1991; Logothetis *et al.*, 1992; Logothetis *et al.*, 1993). Cysteine accessibility studies in *Shaker* channels have shown that the positive charges in S4, when held at a hyperpolarized potential, are either buried in the membrane or cytosol (Larsson *et al.*, 1996). In response to a depolarizing pulse, the S4 segment moves outward and the three most external charges on S4 are exposed to the extracellular solution (this accounts for the 13 $e_0$ in the previous paragraph) (Larsson *et al.*, 1996). There is currently an ongoing controversy as to the exact movement of the S4 segment (paddle vs. helical screw) (Laine *et al.*, 2003; Gandhi *et al.*, 2003; Jiang *et al.*, 2003a; Jiang *et al.*, 2003b).

Although the S4 TM segment in voltage-gated channels has been proposed to be the main voltage sensing mechanism, the potential role of S1, S2 or S3 as sensors is poorly understood. Although there is some data to support the role of S1 and S3 in charge screening, there is some experimental data which suggests that S2 plays an important role in channel activation (Seoh *et al.*, 1996).

How does a change in the conformation of the S4 voltage sensor cause a channel to enter a conducting conformation? A comparison of the crystal structures of the open and closed conformations in MthK and KcsA suggested that a glycine residue in the inner helix (S6) undergoes a conformational, hinge-like, movement with S4 charge displacement that opens the central cavity to the cytoplasm by moving the inner helicies to the periphery of the inner vestibule (Doyle *et al.*, 1998; Jiang *et al.*, 2002; Mackinnon, 2003; Jiang *et al.*, 2003a). However, it has recently been suggested from the crystal structure of Kv1.2 that an interaction between the S4-S5 linker during depolarization

dilates (opens) the inner S6 helices (interaction between S6 and the S4-S5 linker), which opens the permeation pathway to the central cavity (Long *et al.*, 2005).

**Inactivation Gating**

In addition to the process of activation seen in voltage gated potassium channels there is another fundamental process that controls the magnitude and duration of currents (Hodgkin & Huxley, 1952b; Smith *et al.*, 1996). In experiments using the squid giant axon it was observed that there was a rapid decrease of $Na^+$ current following a large depolarization, a phenomenon denoted 'inactivation' (Hodgkin *et al.*, 1952). In sodium channels inactivation is the process that renders channels non-conductive during a sustained depolarization. In Kv channels the process of inactivation regulates and defines the role of channels in their respective tissues. Potassium channels inactivate by at least 2 distinct mechanisms, fast and slow inactivation.

**Fast (N-Type) Inactivation**

The process of fast inactivation is thought to be mediated by the N-terminal region of the channel (Hoshi *et al.*, 1990; Zagotta *et al.*, 1990a). Deletion of the first 20-22 amino acids of the N-terminal region of a *Shaker* $K^+$ channel slowed the rate of inactivation, whereas, application of a peptide comprised of the first 20 amino acids to an inside-out patch restored inactivation in *Shaker* channels which had the N-terminus removed (*Shaker*-IR) (Hoshi *et al.*, 1990; Zagotta *et al.*, 1990a). It was subsequently determined that the first 20-22 amino acids comprise the blocking particle of *Shaker* channels, while the next 60 residues make up a 'chain' that tethers the blocking particle to the channel (Hoshi *et al.*, 1990; Zagotta *et al.*, 1990b). Insertion of residues into the 'chain' of the N-terminal peptide slowed the rate of inactivation, whereas, deletion of

residues accelerated the rate of inactivation (Hoshi *et al.*, 1990; Aldrich *et al.*, 1990; Zagotta *et al.*, 1990b).

Homotetrameric *Shaker* channels are, by definition, comprised of 4 identical subunits all of which contain an inactivating peptide. In mutated heterotetrameric channel constructs it was shown that only one inactivating ball was required to cause complete inactivation of Kv channels; however the rate of inactivation was slowed to ¼ of the wild-type rate (Mackinnon *et al.*, 1993). This result suggested that only one ball peptide is required to inactivate the channel and that the other blocking particles are unable to enter after one particle has entered the inner pore (Mackinnon *et al.*, 1993).

Recovery from inactivation is the process by which the ball dissociates from its site at the inner pore. This process occurs in Kv channels when the membrane is repolarized. A heterotetrameric channel construct with only 1 inactivation particle has been shown to recover from inactivation at the same rate as a wild-type homotetrameric channel that contains 4 inactivating particles (Mackinnon *et al.*, 1993). The rate of recovery from N-type inactivation is dependent on the extracellular concentration of $K^+$ suggesting that ions entering the cell are able to displace the inactivation peptide from the intracellular mouth of the pore (Demo & Yellen, 1992).

**Outer Pore Inactivation**

*C-type Inactivation*

In *Shaker* channels, removal of the fast inactivating N-terminal particle, by deleting the first 20-22 amino acids, does not completely relieve channels of inactivation (Hoshi *et al.*, 1991). This second type of inactivation, called slow inactivation, was found to be voltage independent between -25 and +50mV and to act through a mechanism

distinct from that of fast inactivation. It was shown that mutation of a residue in the S6 region of the *Shaker* channel, A463V, affected slow inactivation (Hoshi *et al.*, 1991). The process of slow type inactivation was originally termed C-type inactivation, which is somewhat of a misnomer as it is now thought that slow type inactivation involves a constriction of the outer pore mouth (Hoshi *et al.*, 1991). It has been shown in C-type inactivation, unlike N-type, that all 4 subunits are required for inactivation to occur and that a concerted conformational re-arrangement at the outer pore mouth is involved (Hoshi *et al.*, 1991).

*P-type Inactivation*

A second type of slow inactivation was later described that appeared to be mechanistically distinct from both N and C-type inactivation. In P-type (pore) inactivation, a mutation in the pore of a Kv2.1 chimeric $K^+$ channel (V369K) accelerated the rate of inactivation by a process with properties distinct from those at position 463 in the S6 segment of *Shaker* channels (De Biasi *et al.*, 1993). In P-type inactivation application of external TEA or increasing the $K^+_o$ slowed the rate of, and recovery from, P-type inactivation and paradoxically increased the current magnitude. Application of internal TEA had no effect on the rate of P-type inactivation supporting the hypothesis that it did not involve the inner pore mouth (De Biasi *et al.*, 1993).

It is thought the process of outer pore inactivation is a combination of the previously mentioned processes: C-type and P-type inactivation. During a sustained depolarization the channel will enter into the less stable P-type inactivated state and then, through a slower mechanism, enter a more stable C-type inactivated state (Loots & Isacoff, 1998). The stability of the inactivated state has been proposed to arise from a

interaction between E418, the S4 contact site, and either residue 451 or 452 at the end of P-S6 linker in *Shaker* (Larsson & Elinder, 2000; Loots & Isacoff, 1998). During inactivation the outer pore of the channel undergoes a conformational change that moves G452 away from E418 and involves the formation of a new bond between E418 and V451 (Loots & Isacoff, 1998; Larsson & Elinder, 2000). It is thought that when the bond between E418 and G452 is broken P450 moves out of its position between W434 and W435 (from adjacent subunits) moving Y445 toward the center of the pore. This structural re-arrangement of the aromatic cuff results in a change at the selectivity filter that causes it to collapse and undergo outer pore inactivation (Larsson & Elinder, 2000).

Crystallization of the potassium channel has increased our understanding of the processes that occur at the pore region; however, there is no clear picture of the conformational re-arrangements that underlie slow inactivation as there is no crystal structure of a channel in the inactivated state. It is thought that during outer pore inactivation there is a collapse of the outer pore that causes a conformational re-arrangement that decreases $K^+$ permeability through a constriction mechanism (Yellen *et al.*, 1994; Liu *et al.*, 1996; Loots & Isacoff, 1998; Gandhi *et al.*, 2000).

*Modulation of outer pore inactivation*

Experiments in Kv channels have shown that the rate of outer pore inactivation is slowed with application of external $TEA^+$ (Mackinnon & Yellen, 1990). These results have led to speculation that the process of outer pore inactivation may be occurring at a site adjacent to or at the site where extracellular TEA binds in Kv channels (Mackinnon & Yellen, 1990; Yellen *et al.*, 1991). In *Shaker* channels, with N-type inactivation removed (*Shaker*- IR), it has been shown that the rate of inactivation was accelerated

when an ion with a lower permeability than $K^+$ was the major extracellular ionic species or if the extracellular $K^+_o$ was decreased (Lopez-Barneo *et al.*, 1993). This was further exemplified when an impermeant ion, N-Methyl-D-Glucamine (NMG), was applied to the bath. With extracellular NMG there was a 4-fold increase in the rate of outer pore inactivation. This result supports the earlier hypothesis that interaction at an external site, where $K^+$ ions bind, affects the rate of inactivation in *Shaker* channels by altering the rate at which outer pore re-orientation can occur (Lopez-Barneo *et al.*, 1993). This result can be partially explained by a 'foot-in-the-door' model, which was first used to describe the change in the deactivation kinetics of delayed rectifier currents in the presence of permeant external cations (Swenson & Armstrong, 1981). A foot-in-the-door model can be used to account for the slower rate of inactivation in *Shaker* T449 mutants because in the presence of high $K^+_o$ (140 mM) it is thought $K^+$ slows the rate of inactivation by occupying an outermost $K^+$ binding site that must be vacant for the channel to inactivate (Lopez-Barneo *et al.*, 1993). This same hypothesis has also been suggested to account for the $TEA^+_o$ mediated slowing of the rate of inactivation in Kv channels of human T-lymphocytes (Grissmer & Cahalan, 1989).

*Mutation of Shaker*-IR *T449 affects the rate of outer pore inactivation*

Mutation of residues in the pore region reduces the $TEA^+_o$ sensitivity of Kv channels and thus it was thought that mutations in the pore would affect the process of outer pore inactivation (Grissmer & Cahalan, 1989). In *Shaker* channels, one of the residues that confers $TEA^+_o$ sensitivity is a threonine at position 449, which is located at the outer pore of the channel (Lopez-Barneo *et al.*, 1993). To investigate the role of this residue in *Shaker*, T449 mutants were engineered that altered the charge, size and pH-

dependence of the residue at position 449. Substitution of a charged amino acid (K, R and E) into the outer pore of *Shaker* accelerated the rate of inactivation ~100-fold, whereas, introduction of a valine or tyrosine (large hydrophobic side chain) dramatically slowed inactivation (Lopez-Barneo *et al.*, 1993). In *Shaker*-IR T449 mutants, an increase in the external concentration of $K^+$ slows the rate of inactivation and increases the maximal outward current, an effect that is more prominent with rapidly inactivating mutants (Lopez-Barneo *et al.*, 1993). This result supports the theory that an extracellular site that is sensitive to extracellular TEA and modulated by external $K^+$ affects the rate of inactivation (Lopez-Barneo *et al.*, 1993; Mackinnon *et al.*, 1993).

*Outer pore inactivation can affect the rates of activation and deactivation*

In addition to affecting the rate of outer pore inactivation it has also been shown that mutation of T449 in *Shaker*-IR affects the rate of deactivation and activation (Molina *et al.*, 1998). An increase in $K^+_o$ and application of external TEA slowed activation and deactivation kinetics by a 'foot-in-the-door' mechanism that stabilized the channel in the open state and increased the occupancy of $K^+$ in the pore (Molina *et al.*, 1998). However, it is unclear how these processes are connected as activation/deactivation and inactivation are thought to be intracellular and extracellular processes, respectively.

**hKv1.5: A Kv Channel Fundamental to Atrial Repolarization**

Kv1.5 is a voltage dependent $K^+$ channel that was initially characterized in atrial tissue of the heart and is involved in repolarization of the atrial cardiac action potential (Fedida *et al.*, 1993); however, there is no fast inactivating component (N-terminal peptide) and the outer pore inactivation is slow ($\tau$ = ~1.3s at +40mV, fit to a single exponential) (Fedida *et al.*, 1993; Kehl *et al.*, 2002). In Kv1.5, as in *Shaker*, the size of

the permeating ionic species and elevation of $K^+_o$ slightly decreases the rate of outer pore inactivation (Fedida *et al.*, 1999). Results from experiments with $Cs^+$ as the charge carrier suggest that ions with a larger crystal radius ($Cs^+$ = 1.74 angstroms, $K^+$ = 1.33 angstroms) destabilize the inactivated state, slowing the rate of outer pore inactivation. In wild-type Kv1.5, R487 (the residue analogous to T449 in *Shaker*) does not confer a high sensitivity to block by external TEA (Fedida *et al.*, 1993); however, replacement of the arginine at 487 by a tyrosine (T449Y) makes Kv1.5 sensitive to block by external $TEA^+$. Mutation of the charged residue at position 487 to a tyrosine did not significantly alter the rate of wild-type inactivation in Kv1.5 suggesting that the site of TEA block and modulation of outer pore inactivation may not be associated (Fedida *et al.*, 1999).

*Extracellular acidification*

In wild-type Kv1.5 changing the pH from 7.4 to 6.4 causes a reduction of outward currents and accelerates outer pore inactivation (Steidl & Yool, 1999; Jager & Grissmer, 2001; Kehl *et al.*, 2002). Increasing $K^+_o$ was shown to antagonize the effect of protons on Kv1.5 by increasing the time constant for inactivation and the maximal outward currents at pH 6.4. These results suggest that modulation of $\tau_{inact}$ by $K^+_o$ is relevant in Kv1.5; however, an accelerated time course for inactivation is required to confer the $K^+_o$ sensitivity. In addition to the effects on inactivation and $I_{max}$, external acidification caused a rightward shift of the $V_{1/2}$. From mutational analysis it was determined that protons alter channel properties through 2 separate mechanisms: by binding to a site in the turret, H463, and through a charge screening effect at an unknown site (Kehl *et al.*, 2002)). Mutation of the histidine at position 463 to a glutamine (H463Q) and neutralization of the

charged residue at position 487 (R487V) decreased the sensitivity of Kv1.5 to external acidification but did not affect $V_{1/2}$.

*Time Constant for Inactivation and $[K^+]_o$ Sensitivity of wild-type Kv1.5*

The time constant for inactivation in wild-type Kv1.5 has a small sensitivity to extracellular $K^+$ (Jager & Grissmer, 2001; Kehl *et al.*, 2002); however, with extracellular acidification inactivation is a $K^+_o$ dependent process. Mutation of the residue at position 487 in Kv1.5 to a histidine has been shown to have no effect on the rate of wild-type inactivation at pH 7.4 (Jager & Grissmer, 2001). However, when the extracellular pH is decreased in both wild-type Kv1.5 and Kv1.5 R487H there is an acceleration of the rate of inactivation with 3.5mM and 140 mM $K^+_o$; however, reduction of $K^+_o$ to 0 mM causes the macroscopic conductance to collapse (Jager & Grissmer, 2001; Kehl *et al.*, 2002). Thus, the question arises why is the rate of outer pore inactivation in Kv1.5 at pH 7.4 not sensitive to alterations in $[K^+_o]$; however, when a charge is present at the analogous residue in other Kv channels, Kv1.4 and Kv1.3, there is a $K^+_o$ mediated effect on the rate of inactivation?

In wild-type Kv1.5, mutation of R487 (analogous to T449 in *Shaker*) reduces sensitivity to external protons and substantially decreases the rate of inactivation (with $Na^+$ as the charge carrier). Mutation of H463 in Kv1.5 to a charged residue (R or K) has previously been shown to accelerate the rate of inactivation and make the channel sensitive to changes in $K^+_o$. These results suggest that the turret and outer pore region of Kv1.5, although in different structural regions, may have a synergistic relationship. By this I mean that alterations in the conformation or charge at either of these sites can have a dramatic effect on the kinetics of outer pore inactivation.

The purpose of this thesis was to further investigate this relationship by changing the residues at both H463 (turret of Kv1.5) and R487 (outer pore region of Kv1.5). It has previously been shown that mutation of K533 to a tyrosine in Kv1.4 (analogous to R487 in Kv1.5) makes the *I-V* relationship non-linear (larger inward than outward currents). Despite the differences in the channel kinetics of Kv1.5 and Kv1.4, $K^+_o$ effects on $I_{max}$ and the rate of inactivation, we attempted to replicate this result by neutralizing the charge at position 487 in Kv1.5. We show here that neutralization of R487 in Kv1.5 to a valine (R487V) makes the *I-V* relationship non-linear, with the normalized outward current magnitude smaller than the inward current. The *I-V* relationship of Kv1.5 R487V and Kv1.4 K533Y were similar in their magnitudes of normalized outward current reduction at +120mV (~60% in both channels) when compared to the corresponding value at –120 mV. In an attempt to elucidate the mechanism for the non-linear *I-V* relationship in Kv1.5 R487V we determined the effect of acidification on the outward currents. Using a permeation model, based on the Eyring-rate theory, we have shown that the reduction of the normalized outward current through Kv1.5 might be accounted for by a change in the outer vestibule, which affects the rate at which $K^+$ ions can enter or exit the permeation pathway.

It has previously been suggested that the protonation state of H463 may influence the protonation state of the arginine at position 487 in Kv1.5 (Jager & Grissmer, 2001; Kehl *et al.*, 2002). To further investigate the role of charged residues at these positions we engineered a swap of the residues (Kv1.5 H463R/R487H) to ascertain the change in channel kinetics with a 'permanently' charged residue at position 463 over a wide pH range, and a protonatable residue in the pore of Kv1.5. A swap of the charged residues at

positions 463 and 487 decreased the time constant for inactivation, increased the time constant for recovery from inactivation, and altered the $K^+_o$ sensitivity of $g_{max}$ between pH 6.4-8.4. The results of this section implicate a critical role for H463, in the non-protonated state, by which it stabilizes the open conformation of the inactivated state and that occupancy of an outer site (possibly adjacent to R487 in Kv1.5) by $K^+$ slows the rate at which Kv1.5 will enter the inactivated state. Introduction of a 'permanently' charged residue at position 463 accelerates the rate of inactivation and might encourage either a non-conducting state or decreased single channel conductance at low $K^+_o$. The time constants for inactivation and deactivation were significantly altered by elevating the $[K^+_o]$ to 140mM, implying a 'foot-in-the-door' mechanism may be involved in slowing the rate of channel deactivation and that outer pore inactivation is slowed by occupancy of $K^+$ at it's outer binding site.

The results from this thesis provide further support that a relationship does exist between H463 and R487 in Kv1.5 by which H463 is involved in stabilization of the open conformation of the channel and that occupancy of a binding site near R487 can slow the rate at which destabilization of the open state occurs.

## Methods

Cell Preparation

In the majority of experiments a human embryonic kidney cell line 293 (HEK-293, American Tissue Culture Collection) was used. HEK-293 cells were used because of their ability to express high levels of human Kv1.5 (Kv1.5) (Fedida *et al.*, 1999). At pH 8.4, in the H463R/R487H experiments, a mouse fibroblast tumour cell line (LM) was used because the magnitude of outward currents was typically too large to accurately voltage clamp in HEK-293. The cells were grown in minimal essential medium (MEM) (Invitrogen, Carlsbad, CA, USA) at 37°C in a 5% $CO_2$-air incubator. HEK-293 cells were plated 1 day before transfection on glass coverslips. Kv1.5 in a pcDNA3 vector (2 μg) was co-transfected with 1μg of CD8 DNA and 3 μl of Lipofectamine 2000 (Invitrogen, Carlsbad, CA, USA). After transfection the cells were incubated in MEM supplemented with 10% fetal bovine serum (FBS) for 12 hours, after which the medium was switched to ensure the cells were not further damaged by the Lipofectamine 2000. Transfected cells were identified using CD8 beads, which bound to CD8 antigens on the extracellular surface. CD8 beads were added to cells 30 min before recording, and then washed off with opti-MEM (Invitrogen, Carlsbad, CA, USA). Currents were recorded 14-36 hours after the initial transfection.

In some experiments a stable cell line expressing Kv1.5 was used. This stable cell line was generated by transfecting a 5ml flask of HEK 293 cells with 2 μg of Kv1.5 and 3 μl of Lipofectamine 2000 in MEM. After 2 days of transfection, the medium was switched and Geneticin (0.5 mg/ml) (Invitrogen, Carlsbad, CA, USA) in MEM was added to the flask. pcDNA3 contains a Geneticin-resistance gene and thus only the cells

expressing the vector survive in the Geneticin-MEM media. After 2 weeks of treatment the cells were passaged, and subsequently maintained using conventional cell culture techniques. Single mutations at position 487 to a histidine (R487H), glutamate (R487E) and a lysine (R487K) were made; however, we were unable to express the mutants in either LM or HEK cells.

Mutagenesis

Point mutations of wild-type Kv1.5 in pcDNA3 were generated using a Quikchange Mutagenesis kit (Strategene, La Jolla, CA, USA) to replace the arginine at position 487 by a valine (R487V) or a histidine (R487H) and the histidine at position 463 to an arginine (H463R). The double mutant Kv1.5 H463R/R487H was generated by sub-cloning a fragment containing the Kv1.5 H463R mutant into the hKv1.5 R487H cassette using BstEII and ClaI restriction enzyme sites (New England Biolabs, Beverly, MA, USA). All mutants were sequenced by the Nucleic Acid and Protein Sequencing (NAPS) facility at the University of British Columbia (Vancouver, BC, Canada) to verify the mutations.

Recording Solutions

The standard bath solution contained, in mM: 140 NaCl,, 3.5 KCl, 10 Hepes, 1 $MgCl_2$, 2 $CaCl_2$, 5 Glucose and was adjusted to pH 7.4 with NaOH. For experiments with nominally $K^+$-free media (0 mM $K^+_o$), KCl was replaced with NaCl. For solutions in which the concentration of $K^+_o$ was greater than 3.5 mM, KCl was substituted for NaCl. For experiments in which symmetrical $K^+$ was used, $[K^+_o]=[K^+_i]=140$ mM, the concentration of NaCl was 3.5 mM, and pH was adjusted using KOH. In experiments that investigated the effect of external pH, solutions were buffered with Hepes (pH 7.4), MES

(pH 6.4) and TAPS (pH 8.4). The standard intracellular solution contained, in mM: 130 KCl, 10 EGTA, 10 Hepes, and 4.2 mM $CaCl_2$, pH adjusted to 7.4 with KOH. For the majority of the experiments the intracellular solution contained no added $Ca^{2+}$ as it has previously been shown to block outward currents at $V_m > +50$ mV (Kwan *et al.*, 2004b). Chemicals were obtained from the Sigma Aldrich Chemical Company (Mississauga, ON, Canada).

Recording

Coverslips with attached cultured cells were removed from the incubator directly before experiments, then sectioned and placed into a ~0.5 ml perfusion chamber and perfused with 5ml of solution prior to recording. All experiments were performed with a bath temperature of 22-25 °C. Patch electrodes were pulled from thin-walled borosilicate glass (World Precision Instruments, FL, USA) and had a resistance of 0.5-2.5 MΩ. Voltage clamp experiments were done with an EPC-8 patch clamp amplifier and Pulse + Pulsefit software was used to generate voltage commands and to analyze the data. Whole cell current recordings were used for Kv1.5 H463R/R487H and wild-type Kv1.5; however, an outside-out patch technique was used for the Kv1.5 R487V experiments because the whole cell currents were too large to accurately voltage clamp with the whole cell technique (an outside-out patch is formed by sealing onto a cell and then pulling the electrode away from the cell so that a small patch of the membrane remains attached to the tip of the electrode). Capacitance and series resistance compensation (30-60%) were used. Currents were filtered at 3 kHz (-3 dB, 8-pole Bessel filter) and were digitized at a sampling interval of 10kHz. A 4 mV compensation was used to correct for the liquid-junction potential between the bath and the recording solution. A P/4 leak

subtraction protocol was used (pulse command divided into 4 equal intervals). The holding potential for the leak protocol was –100mV and the protocol was terminated 50 ms before the voltage command at each potential.

After recordings were obtained in control solutions the chamber was perfused with test solution at a flow rate of ~3 ml/min for 4 minutes to remove control solution in the chamber, which has an estimated volume of ~0.5 ml.

Equations

To calculate the $V_{1/2}$ and slope factor ($k$) a single Boltzmann function was used:

$$y = \frac{A}{1 + \exp\left[(V_{1/2} - V)/k\right]}$$

where $y$ is the normalized current, $A$ is the best-fit value to the data points, $V_{1/2}$ is the half-activation voltage (mV), $V$ is the pre-pulse voltage (mV) and $k$ is the slope factor (mV).

Statistical Analysis

A Tukey-Kramer multiple comparisons One-way Anova was used to test the significance of $K^+_o$ and $pH_o$ effects on the time constants for inactivation and deactivation, and the $pH_o$-dependent shifts in the $V_{1/2}$ and $k$ at pH 7.4 and 8.4. At pH 6.4 (because there were only 2 variables, 10 mM and 140 mM $K^+_o$) an un-paired $t$-test was used to test the significance of acidification on the time constant for activation, deactivation, and inactivation, and $K^+_o$-dependent shifts in the $V_{1/2}$ and $k$.

Results

## Part I: The Role of Charged Residues in the Outer Pore Mouth on the *I-V* Relationship of Kv1.5

It has previously been shown that, owing to a positively charged residue at position 533 (K533), Kv1.4 is sensitive to changes in the extracellular concentration of $K^+$ (Pardo *et al.*, 1992). However, despite having a positively charged residue at the analogous position (R487), Kv1.5 is not sensitive to $K^+_o$ at pH 7.4. In Kv1.4 mutation of the lysine at position 533 to a tyrosine (K533Y) caused the instantaneous *I-V* relationship to show strong inward rectification (Ludewig *et al.*, 1993). In the first section of this thesis a similar mutation at position 487 in Kv1.5, R487V, was created to determine if the process of permeation is similar to Kv1.4 or if, like their sensitivities to $K^+_o$, the phenomena are different. We also determined if the protonation state of the histidine at position 463 affected the open channel *I-V* relationship of Kv1.5 R487V.

### In symmetrical $K^+$ wild-type Kv1.5 has a linear instantaneous *I-V* relationship

A representative family of traces in Figure 2A shows the current against time relationship of wild-type Kv1.5 channels with 140 mM $K^+$ extracellular solution at pH 7.4 (for reasons explained below, these recordings were made with an intracellular solution containing no added $Ca^{2+}$ or $Mg^{2+}$). Control currents were generated by pulsing the cells for 10 ms from a holding potential ($V_H$) of –80 m*V* to +140 mV to open the channels and allow $K^+$ ions to permeate. The membrane was then repolarized to test potentials between –120 and +140 mV in +10 mV increments for 20 ms to record the instantaneous amplitude of the tail currents (Figure 2A). A graph of the peak tail current against the voltage generated a linear *I-V* relationship in wild-type Kv1.5 (Figure 2B) that intersected the 0 current line at 0 mV, the expected $E_{rev}$ for symmetrical $K^+$. The peak tail

current was determined by fitting the decay phase of the current to a single exponential and extrapolating the amplitude at time 0 of the repolarizing pulse. The current amplitude was normalized with respect to the absolute value of the tail current at –120 mV. The normalized current at +120 mV was ~ 1, indicating that the currents were equal but opposite to that at –120 mV and that the open channel *I-V* relationship shows no rectification.

**Kv1.5 R487V has a non-linear *I-V* relationship with symmetrical 140 mM $K^+$ at $pH_o$ 7.4**

In Figures 3A and B representative traces show the currents generated in outside-out patches containing symmetrical $K^+$ with the standard intracellular solution. Currents were generated by pulsing from a holding potential of –80 mV to +140 mV for 10 ms and then to test potentials between –120 and +140 mV for 20 ms in +10 mV increments. It has been previously shown in our lab that at a $V_m$ > +50 mV $Ca^{2+}_i$ causes a rapid pore block (Swenson and Armstrong 1981; Kwan *et al.*, 2004b) and we found a similar effect of $Ca^{2+}_i$ in this experiment. With $Ca^{2+}_i$ we observed an inward rectification of currents, as shown by the lack of changes in the outward current magnitude at voltages above +50 mV, despite the increase in driving force. As a result we switched to an intracellular solution that contained no added $Mg^{2+}_i$ or $Ca^{2+}_i$ (all subsequent recordings were made with no added intracellular $Ca^{2+}$ or $Mg^{2+}$). In Figure 3C, analysis of the tail current amplitude generated an *I-V* relationship that behaved in a manner similar to that of Kv1.4 K533Y. When the absolute current amplitude was normalized to –120 mV, the current at +120 mV was 0.38 (0 $Ca^{2+}_i$) ($n$=7) and 0.17 (50 nM free $Ca^{2+}_i$) ($n$=3) of the normalized current.

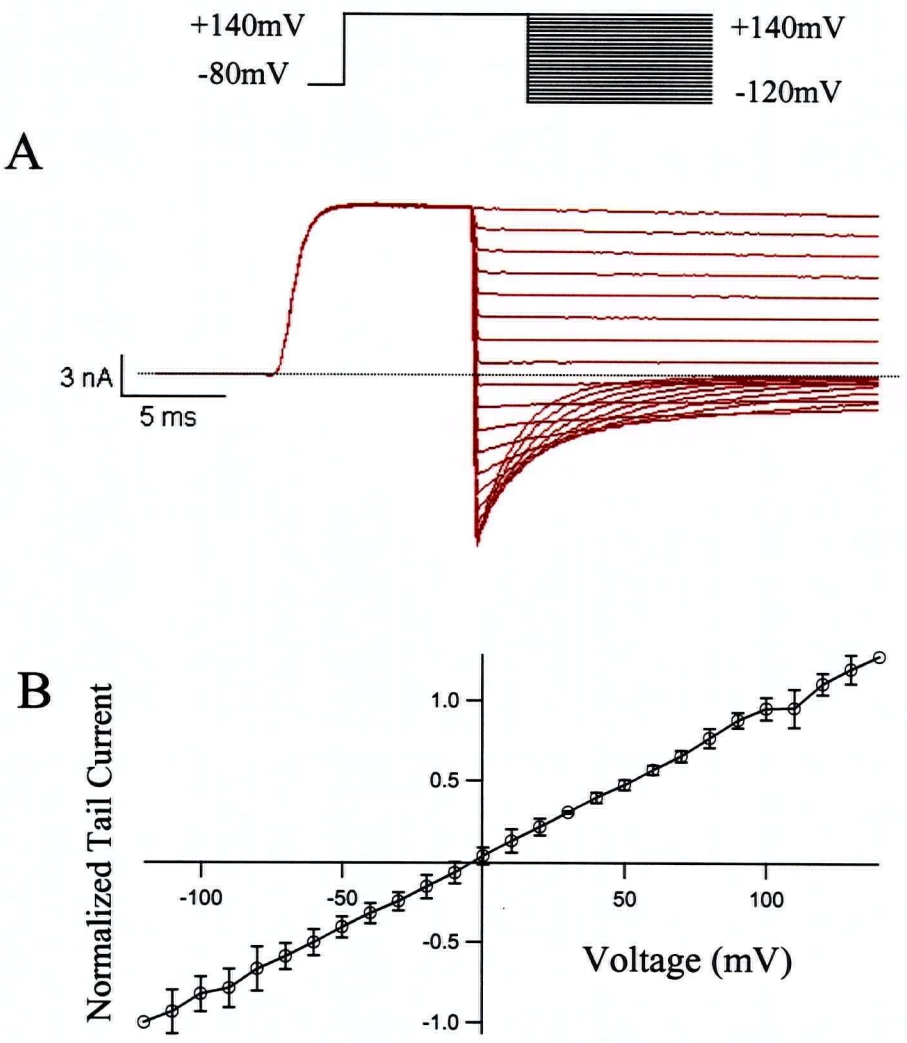


Figure 2 **The instantaneous *I-V* relationship of wild-type Kv1.5 with symmetrical 140 mM $K^+$ is linear.** **A**, Representative traces show the current generated with a pulse from a holding potential of -80 mV to +140 mV for 10 ms followed by repolarization to a voltage between –120 and +140 mV for 20 ms. Recordings were done in a symmetrical $K^+$ solution that contained no added intracellular $Mg^{2+}$ or $Ca^{2+}$. **B**, Analysis of tail current amplitude generated an instantaneous *I-V* relationship in which the current elicited at –120 mV was approximately equal and opposite to the current at +120 mV. Normalization of the *I-V* relationship with respect to the absolute value for the tail current at –120 mV produced a linear relationship in which the normalized current at +120 mV was ~1 ($n$=4).

In Figure 3D, a merged *I-V* relationship of wild-type Kv1.5 (Figure 2B) and Kv1.5 R487V (0 M $Ca^{2+}_i$) (Figure 3C) shows that the *I-V* relationship at negative potentials is similar in wild-type Kv1.5 and Kv1.5 R487V, however the magnitude of the normalized outward current is smaller in Kv1.5 R487V. In Kv1.4 K533Y it was shown that the *I-V* relationship was non-linear because the magnitude of the single channel inward currents was larger with neutralization of the charge at position 533. However, because we have not done single channel recordings in Kv1.5 R487V we can't conclusively say if a change in the outward or inward current magnitude accounts for the change of the *I-V* relationship.

**Current magnitude and the *I-V* relationship are both pH-insensitive in hKv1.5 R487V**

It has previously been shown in Kv1.5 that mutation of the arginine at position 487 to a valine (R487V) decreases the sensitivity to extracellular acidification (Kehl *et al.*, 2002). In wild-type Kv1.5 there is a histidine residue at 463 (H463), which, at pH 6.4, will be partially protonated. The next experiment was designed to determine if the protonation state of the histidine at 463 would affect the permeation process through Kv1.5 R487V. In Figure 4A, representative traces show the current generated in an outside-out patch with symmetrical 140 mM $K^+$ at pH 6.4 (red) ($n$=4), pH 7.4 (black) ($n$=7) and pH 8.4 (blue) ($n$=3). Currents were generated by pulsing from a holding potential of –80 mV to +140 mV for 10 ms, followed by a repolarizing step to -120 mV for 20 ms. From Figure 4A it was concluded that there was no significant change in either the current amplitude or deactivation kinetics at –120 mV when the external pH was switched between 6.4 and 8.4.

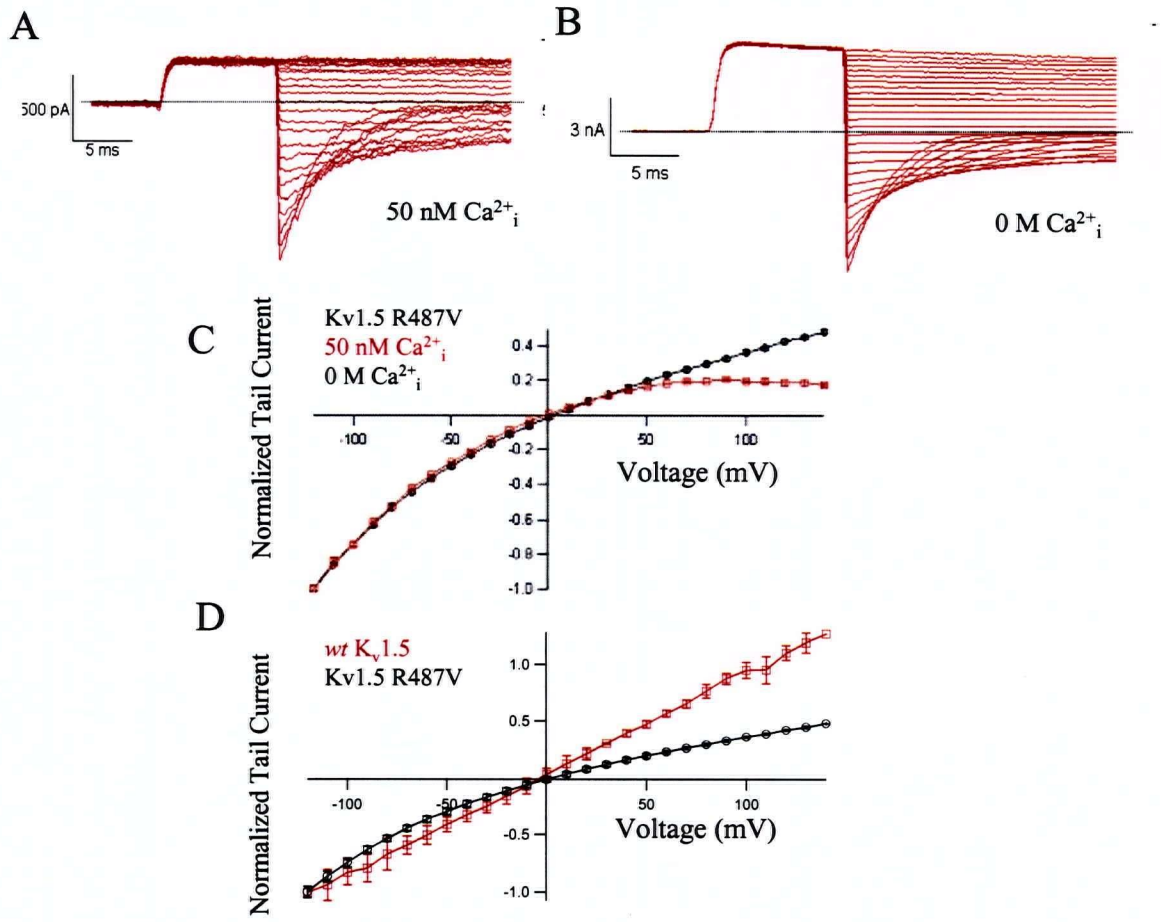


Figure 3 **In symmetrical 140 mM $K^+$ the instantaneous *I-V* relationship of Kv1.5 R487V is non-linear. A & B**, Representative current traces were generated by pulsing from a holding potential of -80 mV to +140 mV for 10 ms followed by repolarization to a voltage between -120 and +140 mV, in +10 mV increments, for 20 ms. **C**, Analysis of tail current amplitude generated an *I-V* relationship in which the current magnitude at -120 mV was approximately 2.17 times the value at +120 mV (0 mM free $Ca^{2+}_i$). Normalization of the *I-V* relationship to the value for the tail current at –120 mV produced a non-linear relationship in which the normalized current at +120 mV was 0.38 (0 $Ca^{2+}_i$) (*n*=7) and 0.17 (50nM $Ca^{2+}_i$) (*n*=3) of the value at –120 mV. **D**, Normalized *I-V* relationship with symmetrical $K^+$ in wild-type Kv1.5 (red) and Kv1.5 R487V (black). The *I-V* relationship in the R487V mutant has a decreased slope conductance between -90 and -40 mV when the currents are normalized to –120 mV, and at $V_m$> 0 mV there is 2.17 fold reduction in the normalized current at +120 mV.

In Figure 4B, normalization of the instantaneous tail current amplitude with respect to the peak current at -120 mV generated an *I-V* relationship similar to Figure 3C for all pH values. This result suggests that the protonation state of the histidine at position 463 (H463), which has a $pK_H$ of ~6.2 (Perez-Cornejo *et al.*, 1999; Kehl *et al.*, 2002) does not have a significant effect on the rate of $K^+$ exit or entry from the extracellular mouth of the pore.

**Modeled data of the *I-V* relationship of hKv1.5 and hKv1.5 R487V with 140 mM $K^+_o$**

Figure 5A shows the symmetrical energy profile of a permeation model, based on Eyring-rate theory, which was used to investigate the changes in the instantaneous *I-V* relationship that resulted from mutation of a charged residue at position 487 in Kv1.5. In the model, the outer and inner energy barriers were 5 *RT* units (p1a and p3a), the inner and outer energy wells (or $K^+$ binding sites) were –9 *RT* units (s1a and s2a), and a transition barrier of –6 *RT* units (s2a) regulated the flux between the 2 binding sites. There was no repulsive factor included in the model (see Discussion for a justification of these parameters). In Figure 5B experimental data (from Figures 2B and 3C) show the *I-V* relationship with symmetrical $K^+$ in wild-type Kv1.5 (red trace) and Kv1.5 R487V (black trace). In Kv1.5 there is a linear *I-V* relationship with symmetrical 140 mM $K^+$; however, in Kv1.5 R487V, under the same conditions, the magnitude of the normalized outward current at +120 mV is ~2.17-fold smaller than the inward current at –120 mV. Figure 5C shows the *I-V* relationship of the current generated in the permeation model with symmetrical $K^+$ (red trace) and the relationship when the outer energy barrier is increased by 1 *RT* unit (black trace).

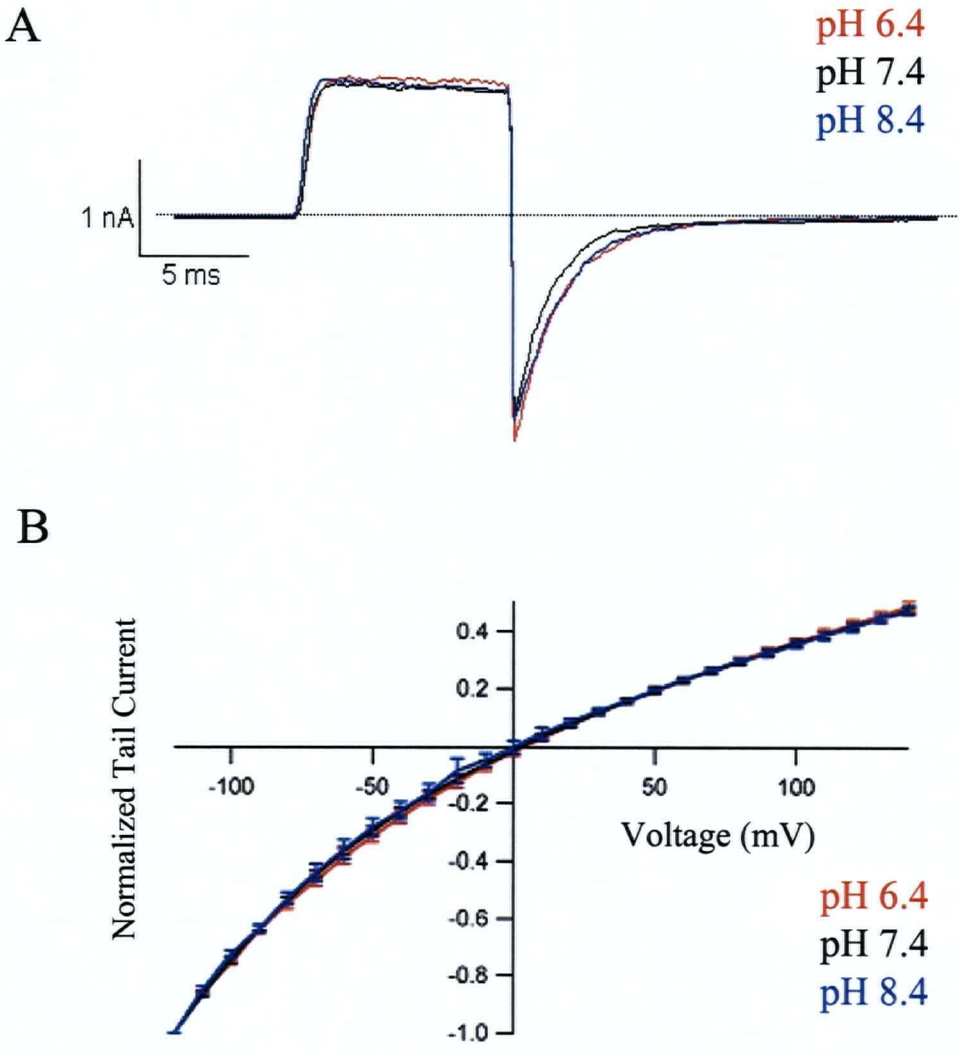


Figure 4 ***I-V* Relationship of Kv1.5 R487V is not pH sensitive.**
**A,** Representative current traces, at pH 6.4 (red) ($n$=4), pH 7.4 (black) ($n$=7) and pH 8.4 (blue) ($n$=3), were generated by pulsing from a holding potential of –80 mV to +140 mV for 10 ms followed by a repolarization to -120 mV for 20 ms. There was no significant difference in the rate of deactivation, or the peak outward and inward current with extracellular acidification. B, Analysis of the instantaneous tail current amplitude produced an *I-V* relationship where the normalized current elicited at –120 mV was approximately 2.17 times larger than the current at +120 mV for pH 6.4, 7.4 and 8.4. This result supports the previous finding that Kv1.5 R487V reduced pH sensitivity, and suggests that the protonation state of H463 does not affect the rate of $K^+$ exit or entry from the outer pore mouth.

From the result in Figure 5C (black trace) it is evident that increasing the height of the outer barrier can accurately replicate both the reduction of the normalized outward current at positive voltages and the decrease in the slope conductance between -90 and -50 mV. The non-linear *I-V* relationship and the decreased slope conductance were also replicated by making the depth of the outer $K^+$ binding site more negative (-10 *RT* units). This result suggests that a change of the outer pore mouth is capable of altering the rate of permeation through Kv1.5 R487V.

In this section I have shown that in Kv1.5 R487V there is a reduction of the normalized outward current, in comparison to the absolute current at –120 mV, with symmetrical $K^+_o$ and a decrease in the slope conductance between -90 and -40 mV. In an attempt to explain these findings we have used a model applied to Kv1.4 by Heinemann's group (Ludewig *et al.*, 1993) in which the height of the outer energy barrier and the depth of the outer binding site were increased or decreased, respectively, by 1 *RT* unit. This result suggests that a change in the outer pore of the channel is decreasing the outward flux of $K^+$ at positive voltages.

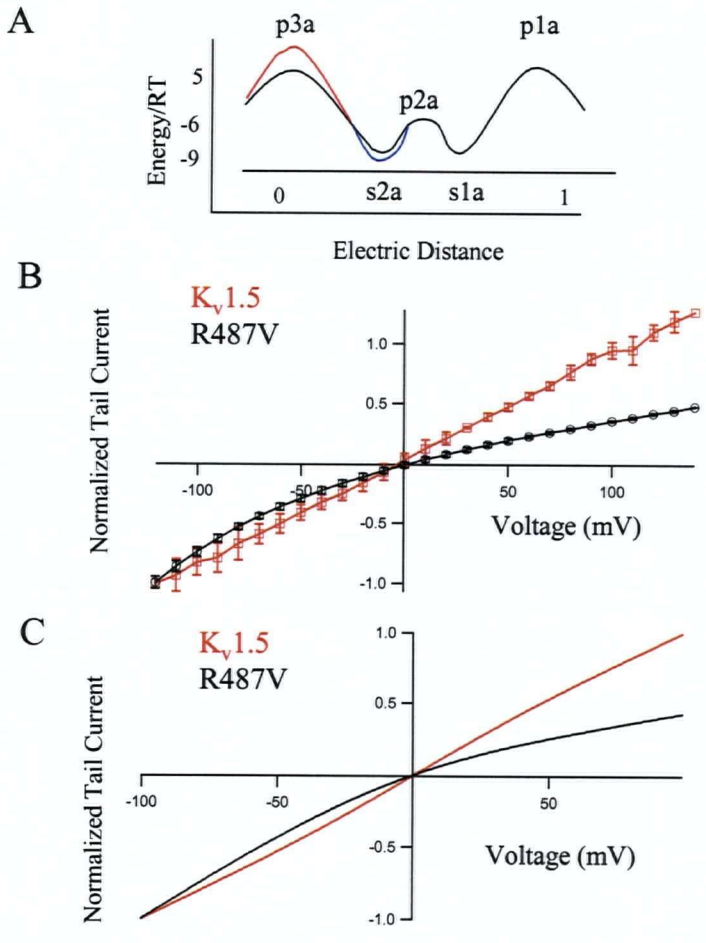


Figure 5 **The instantaneous *I-V* relationship of a permeation model, based on Eyring-rate theory, replicates the experimental data from Kv1.5 and Kv1.5 R487V.** **A,** A symmetrical pore with 2 binding sites (no repulsive factor) was used to investigate the mechanism by which a mutation at residue 487 causes the *I-V* relationship of Kv1.5 to inwardly rectify. The heights of the free energy profile of the model was determined using previously reported values (Ludewig *et al.*, 1993) and the knowledge that single channel current of Kv1.5 at +100 mV is ~1.5pA (data not shown) (Kwan *et al.*, 2004b). P3a, p2a and p1a represent the external, transitional and internal energy barriers, respectively; whereas, s2a and s1a are the external and internal binding sites, respectively. **B**, Experimental data from Kv1.5 and Kv1.5 R487V in symmetrical $K^+_o$ shows that mutation of the arginine at 487 causes the normalized outward current to be ~2.17-fold smaller than the absolute current at –120 mV. **C**, In the Eyring-rate model, with symmetrical $K^+_o$, the *I-V* relationship is linear (analogous to the wild-type Kv1.5 *I-V* relationship). In an attempt to replicate the change in permeation that results from the R487V mutation, the outer free energy barrier (red) and outer binding site (blue) of the permeation pathway were increased and decreased, respectively, by 1 *RT* unit. This caused a significant reduction in the magnitude of the normalized outward current when compared to inward current and a reduction of the slope conductance at negative voltages. The result obtained in this section supports the hypothesis that a change at the outer vestibule is decreasing the rate at which $K^+$ ions are able to vacate the pore.

## Part II: The effect of $K^+_o$ and $pH_o$ on the macroscopic channel kinetics of Kv1.5 H463R/R487H

### $K^+_o$ and $pH_o$ dependence of H463R/R487H

In Kv1.5 there is a protonatable histidine group at position 463 ($pKa$ = ~6.2) of the turret, and a positively charged arginine at position 487 ($pKa$ = ~10.5) near the outer pore mouth. It has previously been shown that mutation of these residues can decrease the sensitivity of Kv1.5 to extracellular acidification, change the time constant for inactivation and affect channel availability as evidenced by a change of $g_{max}$. In this section of the thesis we mutated the residue at position 463 to an arginine (H463R) and the arginine at position 487 to a histidine (R487H). This mutant allowed us to ascertain current behavior with a residue in the turret assumed to be positively charged over a wide pH range and a protonatable residue at the outer pore mouth.

### $I_{max}$ is dependent on $K^+_o$ and pH

In Figures 6A, C and E representative current traces from different cells at pH 6.4, 7.4, and 8.4 show the pH dependence of Kv1.5 H463R/R487H. Currents were elicited by pulsing from a holding potential of –80 mV to +50 mV for 300 ms to allow inactivation to proceed to a steady-state, and then repolarizing to –50 mV for 100 ms. In wild-type Kv1.5, at pH 7.4, raising or lowering $K^+_o$ does not affect $I_{max}$ (other than through changes in the driving force) (Kehl *et al.*, 2002) however, at pH 6.4, 7.4 and 8.4 in Kv1.5 H463R/R487H there was an obvious correlation between the magnitude of the peak current ($I_{max}$) at +50 mV and the extracellular concentration of $K^+$.

At pH 6.4 (Figure 6A), the currents generated with 0 or 3.5 mM $K^+_o$ were not readily discernable from the endogenous currents in HEK-293 cells. Elevation of the extracellular concentration of $K^+$ to 10 and 140 mM elicited currents that were 1.8 nA

and 2.5 nA, respectively. The current with 140 mM $K^+_o$ was ~30% larger than 10 mM $K^+_o$ despite the large reduction in the driving force. This result suggests that by lowering $pH_o$ there is a shift of the $[K^+]_o$ required for half-maximal channel availability, assuming the effect of protons on Kv1.5 H463R/R487H resembles that of wild-type Kv1.5 (Kwan et *al.*, in review). In addition, it is implied that with 0 and 3.5 mM there is a high proportion of channels unavailable which have no discernable current, but that increasing the $K^+_o$ stabilizes the open conformation and increases the proportion of available channels. From these data it is not apparent what concentration of $K^+_o$ is required to maximize channel availability as the currents at 140 mM $K^+_o$ are larger than the other concentrations, despite the reduction in driving force (Figure 6A).

At pH 7.4 (Figure 6C), there are currents with 0 mM, 3.5 mM, 10 mM and 140 mM $K^+_o$. In 0 mM $K^+_o$ $I_{max}$ is 6-fold smaller than the outward current with 3.5 mM $K^+_o$. However, when the extracellular concentration of $K^+$ is increased to 10 mM or 140 mM, the current magnitude at +50 mV is 1.75 and 2.1-fold larger, respectively, than at 3.5 mM $K^+_o$. This result indicates that a large proportion of channels might be in an unavailable state at pH 7.4 (see previous paragraph) with 0 mM and 3.5 mM $K^+_o$. It is unknown what concentration of $K^+_o$ is required for the channels to be fully available because even though the $I_{max}$ with 140 mM $K^+_o$ is smaller than with 10 mM, the lower driving force with 140 mM $K^+_o$ makes a meaningful comparison impossible. However, based on the $K^+_o$ concentrations used in this experiment it can be suggested that the $K_D$ for channel availability is between 3.5 mM and 140 mM $K^+_o$.

At pH 8.4 (Figure 6E), the $K^+_o$ dependence of channel availability was similar to that of pH 7.4, with a $K_D$ estimated to be between 3.5 mM and 140 mM (Figure 6E). The

most noticeable difference between the responses at pH 8.4 and pH 7.4 was the increase in the $I_{max}$ with 0 mM $K^+_o$ compared to the $I_{max}$ with 3.5 mM $K^+_o$. At pH 7.4, there was a 6-fold difference between the $I_{max}$ with 0 mM and 3.5 mM $K^+_o$; however, at pH 8.4 there was only a 2-fold difference in these parameters. This result exemplifies an important trend observed in Figures 6A, C and E in which there was a reduction in the $K^+_o$ required to make the channels fully available as the pH was increased from 6.4 to 8.4.

**Accelerated inactivation in Kv1.5 H463R/R487H**

At pH 6.4, 7.4 and 8.4 (Figures 6B, D and F) the most striking change in the kinetics of the Kv1.5 H463R/R487H mutant, in comparison to wild-type kinetics, was the accelerated inactivation at pH 7.4 with 3.5 mM $K^+_o$. The time constant for inactivation in wild-type Kv1.5 typically fits much better to a double exponential, however, for this mutant a better fit was obtained with a single exponential. The time constant for inactivation of Kv1.5 H463R/R487H is further characterized in a subsequent section.

**$K^+_o$ and pH dependence of *g-V* relationship in H463R/R487H**

Panels of A, C and E of Figure 7 show current traces generated at pH 6.4 (140 mM $K^+_o$), 7.4 (3.5 mM $K^+_o$) and 8.4 (10 mM $K^+_o$) when the holding potential was stepped from –80 mV to voltages between –30mV and +50 mV in 10 mV increments for 15 ms, and then returned to a voltage of -40 mV for 20 ms. The aim of these experiments was to determine the half activation voltage ($V_{1/2}$) and slope factor ($k$) of Kv1.5 H463R/R487H with different pH and $K^+_o$ values. This analysis was motivated by the fact that activation has been shown to be affected by the charge on residues in the turret of Kv channels (Elinder *et al.*, 1996).

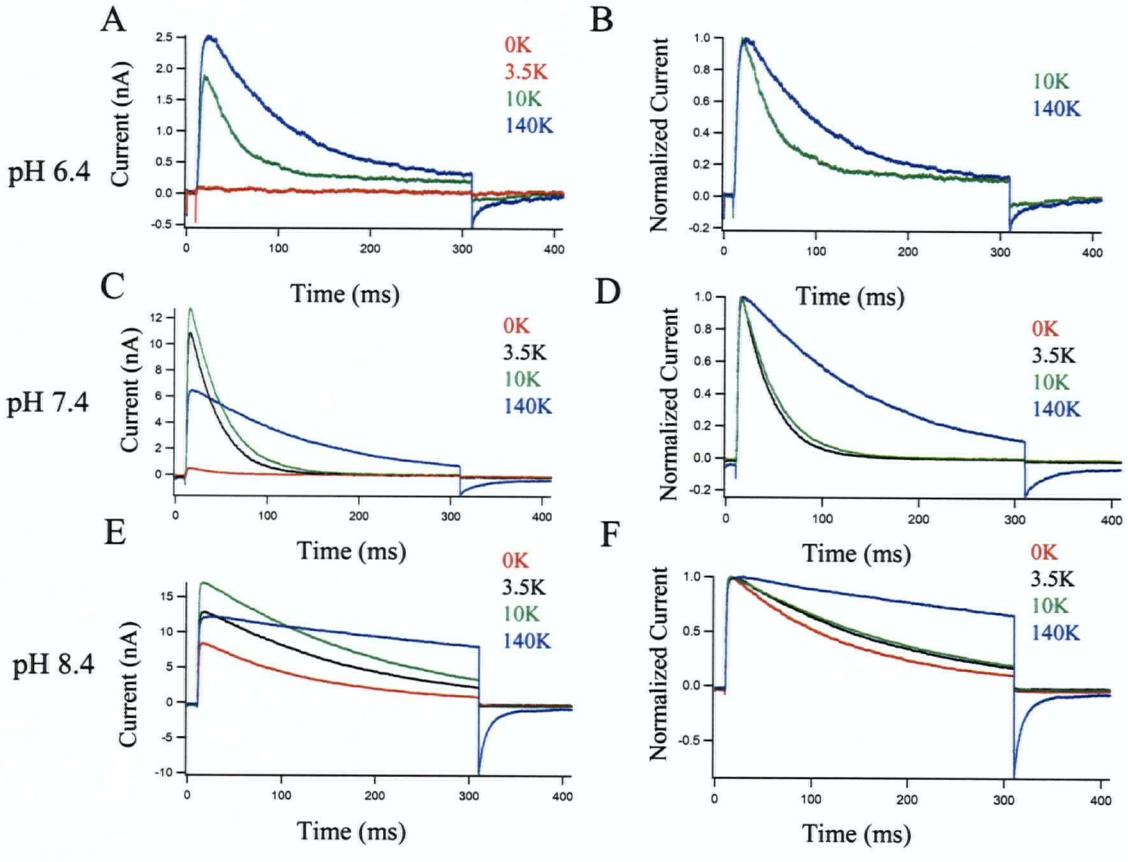


Figure 6 $I_{max}$ **in Kv1.5 H463R/R487H is pH (6.4, 7.4, and 8.4) and $K^+_o$ sensitive (140 mM). A, C and E** Representative traces show the current generated when different cells at pH 6.4, 7.4, or 8.4 were pulsed from a holding potential of –80 mV to +50 mV for 500 ms followed by a repolarization to –40 mV for 100 ms. The effect of 0 mM (red), 3.5 mM (black), 10 mM (green) and 140 mM $K^+_o$ (blue) at pH 6.4, 7.4 and 8.4 were investigated. The $K_D$ for channel availability was not determined; however, based on the $I_{max}$ at pH 6.4, 7.4 and 8.4 ~ 140 mM, 10 mM and 10 mM, respectively, was required for maximal channel availability. This result suggests that the proportion of channels available for activation in Kv1.5 H463R/R487H is both pH and $K^+_o$ dependent. **B, D and F** Normalized currents at pH 6.4, 7.4 and 8.4 show the change of the time constant for inactivation with a $K^+_o$ of 0 mM (red), 3.5 mM (black), 10 mM (green) and 140 mM (blue). At pH 6.4 there was no measurable current at 0 mM and 3.5 mM $K^+_o$. From the 3 normalized traces (pH 6.4, 7.4 and pH 8.4) it is apparent that a $K^+_o$ of 140 mM causes a significant increase in $\tau_{inact}$ when compared to the other $[K^+]_o$.

A *g-V* curve for each pH value and [$K^+_o$] was determined by fitting the tail currents to a single exponential function at -40 mV and plotting the normalized peak tail current against the corresponding voltage.

In Figures 7B, D and F normalized *g-V* curves show the effect of $K^+_o$ at each pH. The data were fitted to a single Boltzmann function (see Methods) to obtain the slope factor ($k$) and half-activation voltage ($V_{1/2}$).

At pH 6.4 (Figure 7B) there was no estimate of the $V_{1/2}$ or $k$ for 0 or 3.5 mM $K^+_o$ because there were no measurable currents. In 10 mM and 140 mM $K^+_o$ the $V_{1/2}$ and $k$ were 4.4 ± 0.5 mV and 4.4 ± 0.4 mV ($n$=3), 4.8 ± 0.2 mV and 6.8 ± 0.2 mV ($n$=4), respectively. There was no significant difference in the $V_{1/2}$ or $k$ at pH 6.4 between 10 mM and 140 mM $K^+_o$.

At pH 7.4 (Figure 7D) the $V_{1/2}$ and $k$ for 0 mM, 3.5 mM, 10 mM and 140 mM $K^+_o$ were –6.7 ± 0.6 mV and 6.9 ± 0.8 mV ($n$=3), -2.3 ± 0.5 mV and 7.8 ± 0.5 mV ($n$=4), -1.3 ± 0.7 mV and 7.2 ± 0.6 mV ($n$=3), and 8.7 ± 0.7 mV and 8.0 ± 0.6 mV ($n$=3), respectively. At pH 7.4, there was no significant difference between the $V_{1/2}$ and $k$ in comparison to the values at pH 6.4 (10 mM and 140 mM $K^+_o$), or when comparing the $V_{1/2}$ or $k$ with 0 mM, 3.5 mM, 10 mM and 140 mM at pH 7.4.

At pH 8.4 (Figure 7F), there was a leftward shift of the $V_{1/2}$ and an increase in the slope factor, $k$, when compared to pH 7.4. At 0 mM $K^+_o$ the $V_{1/2}$ and $k$ were –5.9 ± 1.1 mV and 8.8 ± 1.0 mV ($n$=3) respectively, with 3.5 mM, 10 mM and 140 mM $K^+_o$ the values for $V_{1/2}$ and $k$ were -8.3 ± 0.5 mV and 7.6 ± 0.5 mV ($n$=4), -8.4 ± 0.7 mV and 7.9 ± 0.7 mV ($n$=3), and –24.7 ± 0.4 mV and 5.1 ± 0.4 mV ($n$=4). The change between pH 8.4 and 7.4 in $V_{1/2}$ and $k$ were the most striking at 140 mM $K^+_o$ where there was a 32 mV

shift of the $V_{1/2}$, in the hyperpolarizing direction and approximately a 2-fold reduction in $k$, indicating that at pH 8.4 the channels open at less depolarized potentials and are more sensitive to changes in voltage. At pH 8.4, the $V_{1/2}$ and $k$ were significantly different with 140 mM when compared to the values with 0 mM, 3.5 mM and 10 mM $K^+_o$. With 0, 3.5 and 10 mM there was no significant difference in either the $V_{1/2}$, or the slope factor between pH 7.4 and 8.4.

**$K^+_o$ and pH dependence of $\tau_{act}$ of H463R/R487H**

Figure 8A, C and E show representative currents at pH 6.4 (140 mM $K^+_o$), 7.4 (140 mM $K^+_o$) and 8.4 (10 mM $K^+_o$) evoked by stepping from a holding potential of -80 mV to voltages between -40 mV and +50 mV for 500 ms and then repolarizing to -40 mV for 300 ms. The $\tau_{act}$ was estimated by fitting the rising phase of the currents generated by the pulses from -40 to +50 mV to a single exponential function.

Figure 8B, D, and F shows the $\tau_{act}-V$ curves at pH 6.4, 7.4, and 8.4. The data points were fit to a single exponential function which shows the e-fold change/mV between -10 and +40 mV. Values for the e-fold change/mV were not determined as many of the data points fit poorly to a single exponential function.

At pH 6.4 (Figure 8B), $\tau_{act}$ with 140 mM $K^+_o$ ($n$=3) was ~1.15-fold larger than with 10 mM ($n$=3) $K^+_o$ at +40 mV. There was no significant difference in the time constant for activation at +40 mV with 10 mM and 140 mM $K^+_o$ at pH 6.4. It is possible that this result was not significant because of the low sample numbers with this mutant. At +40 mV, there was no significant difference in the $\tau_{act}$ between 10 and 140 mM $K^+_o$.

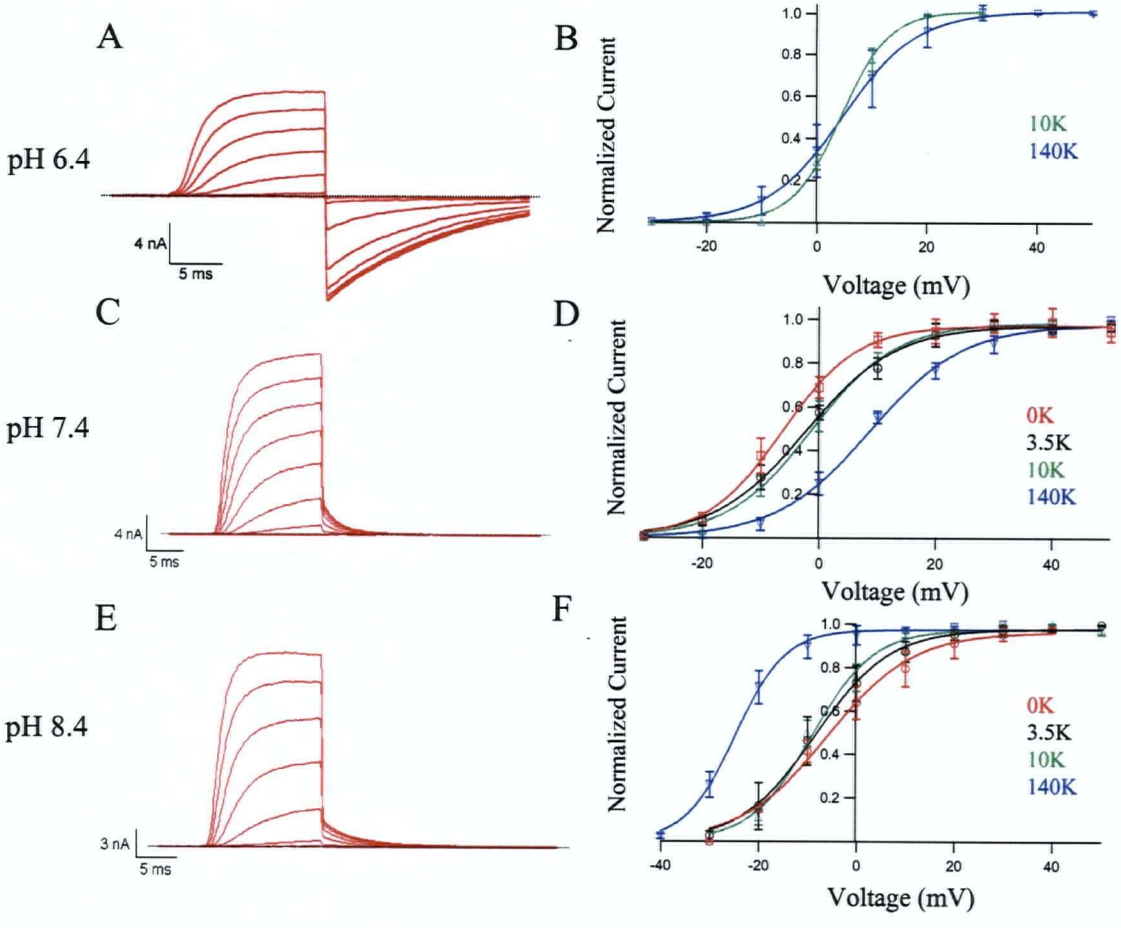


Figure 7 **The slope factor and half-activation voltage of Kv1.5 H463R/R487H shows pH and $K^+_o$ dependence. A, C and E** Representative traces show the current generated when different cells at pH 6.4 (140 mM $K^+_o$), 7.4 (10 mM $K^+_o$), or 8.4 (3.5 mM $K^+_o$) were pulsed from a holding potential of –80 mV to voltages between -30 mV and +50 mV for 15 ms and then repolarized to –40 mV for 20 ms. The tail currents at –40 mV were fitted to a single exponential function to determine the conductance as a function of voltage. **B, D and F** *g-V* curves are both pH dependent (depolarizing shift with acidification) and $K^+_o$ dependent (34mV shift when the pH was increased from 7.4 to 8.4 with 140 mM $K^+_o$). Extracellular $K^+$ concentrations of 0 mM (red), 3.5 mM (black), 10 mM (green) and 140 mM (blue) were used to determine if the voltage dependence of activation ($V_{1/2}$) or the slope factor ($k$) were affected by changing the $K^+_o$.

At pH 7.4 (Figure 8D), the time constant for activation with 0 mM ($n$=4), 3.5 mM ($n$=7), 10 mM ($n$=3) and 140 mM $K^+_o$ ($n$=3) were approximately equal at +40 mV. There was found to be no significant difference in the rates of activation at pH 7.4 with all of the concentrations of $K^+_o$ tested.

At pH 8.4 (Figure 8F) there was again no significant difference between $\tau_{act}$ with 0 mM ($n$=3), 3.5 mM ($n$=4), 10 mM ($n$=3) or 140 mM $K^+_o$ ($n$=4) at +40 mV in Kv1.5 H463R/R487H.

From the results presented in Figure 8, it was apparent that the time constant for activation was not significantly affected by changing the $K^+_o$ at pH 6.4, 7.4 or 8.4 in Kv1.5 H463R/R487H at +40 mV. Therefore, it can be assumed that the changes in the time constant for inactivation (see subsequent section) and $I_{max}$ do not result from a change in the activation of Kv1.5 H463R/R487H.

**$K^+_o$ and pH dependence of $\tau_{inact}$ of H463R/R487H**

The time constant for inactivation was determined by fitting the current decay in traces such as those shown in Figures 8A, C and E to a single exponential function. Panels A, B and C of Figure 9 show the time constant for inactivation against the voltage at pH 6.4, 7.4 and 8.4 with 0 mM, 3.5 mM, 10 mM and 140 mM $K^+_o$. This analysis was undertaken to determine if the time constant for inactivation is $K^+_o$ dependent in the Kv1.5 H463R/R487H. The data points in Figure 9, based on data from 3-7 cells, were fit with a single exponential function to approxaimte the e-fold change/mV of the time constant for inactivation. Values for the e-fold change/mV were not determined as many of the data points fit poorly to a single exponential function and thus no meaningful comparison could be inferred.

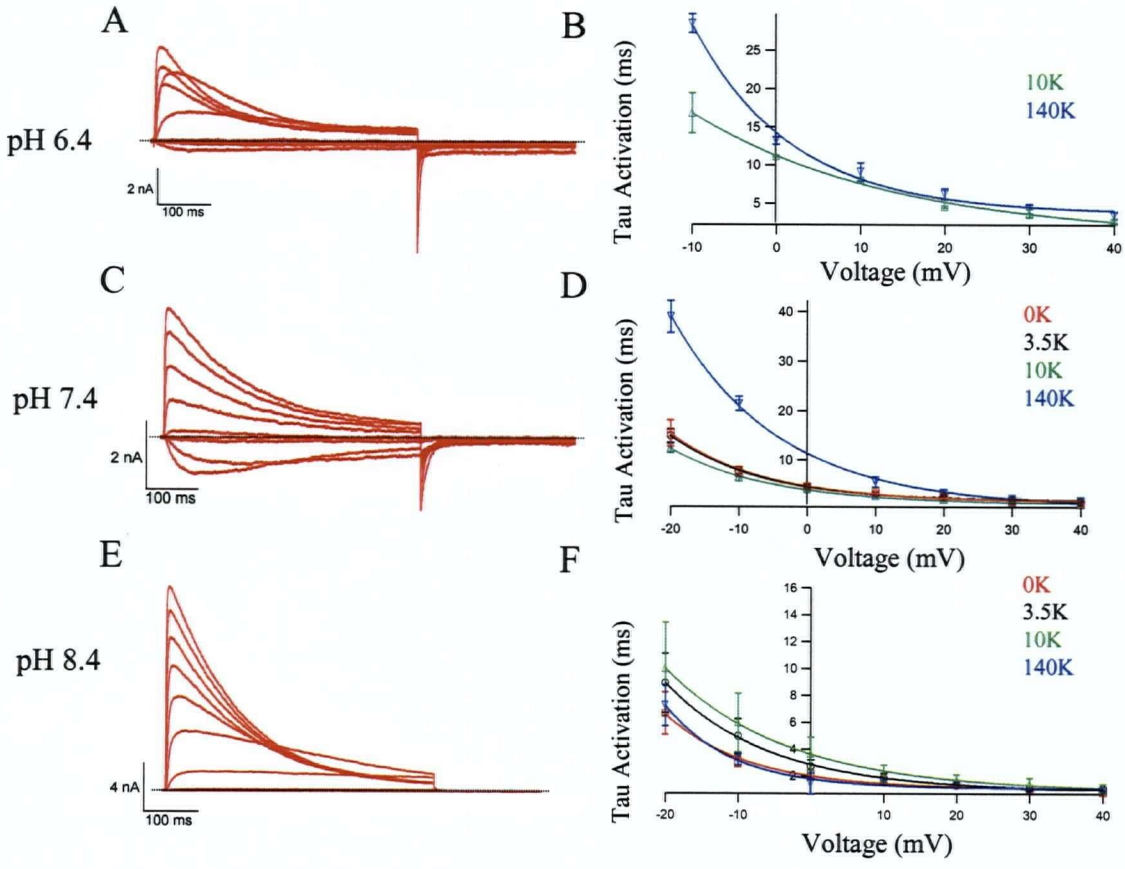


Figure 8 **The time constant for activation in Kv1.5 H463R/R487H is not $K^+_o$ sensitive. A, C and E** Representative traces at pH 6.4 (140 mM $K^+_o$), 7.4 (3.5 mM $K^+_o$), or 8.4 (140 mM $K^+_o$) were generated by pulsing from a holding potential of –80 mV to voltages between -30 mV and +40 mV for 500 ms and then to -40 mV for 300 ms. The rising phase of the current was fitted to a single exponential to approximate the rate of activation. **B, D and F** Analyzed data shows a pH (fastest at pH 8.4) and voltage dependence (smaller $\tau_{act}$ with stronger depolarization) of the time constant for activation. There was no significant difference in the time constant for activation with 0 mM, 3.5 mM, 10 mM or 140 mM $K^+$ at a given pH, or when comparing the values for $\tau_{act}$ at pH 6.4, 7.4 and 8.4.

At pH 6.4 (Figure 9A), the $\tau_{inact}$ at +40 mV with 10 and 140 mM $K^+_o$ was 28.2 ± 1.3 ms ($n$=3), and 91.9 ± 5.2 ms ($n$=3), respectively. The time constant for inactivation at pH 6.4 with 140 mM $K^+_o$ was significantly slower than the inactivation with 10 mM $K^+_o$. The $\tau_{inact}$ of Kv1.5 H463R/R487H at pH 6.4 with 0 mM and 3.5 mM $K^+_o$ was not determined as there was no appreciable current.

At pH 7.4 (Figure 9B) the $\tau_{inact}$ at +40 mV for 0 mM, 3.5 mM, 10 mM and 140 mM $K^+_o$ was 33.8 ± 5.3 ms ($n$=4), 35.9 ± 1.6 ms ($n$=7), 61.3 ± 5.1 ms ($n$=3), and 164.7 ± 21.9 ms ($n$=3), respectively. The increase in $\tau_{inact}$ at +40 mV with 140 mM $K^+_o$ at pH 7.4 in comparison to 0 mM, 3.5 mM and 10mM $K^+_o$ was significant ($p < 0.05$). A comparison of $\tau_{inact}$ showed that an increase of the $pH_o$ from 6.4 to 7.4 increased the time constant for inactivation with both 10 mM and 140 mM $K^+_o$ by ~2-fold.

At pH 8.4 (Figure 9C), there was a significant $K^+_o$ dependence to the rate of inactivation. At pH 8.4 the time constant inactivation at +40 mV was 50.1 ± 14.9 ms ($n$=3), 95.6 ± 12.9 ms ($n$=4), 125.7 ± 5.8 ms ($n$=3), and 489.8 ± 10.9 ms ($n$=2) with 0 mM, 3.5 mM, 10 mM and 140 mM $K^+_o$, respectively. The time course of inactivation with 140 mM $K^+_o$ was determined using longer pulse durations (+40 mV for 2000 ms) to account for the significantly larger time constant of inactivation. In agreement with the results at pH 6.4 and 7.4, there was a significant increase in $\tau_{inact}$ at pH 8.4 with 140 mM $K^+_o$, when compared to the other $K^+_o$ concentrations.

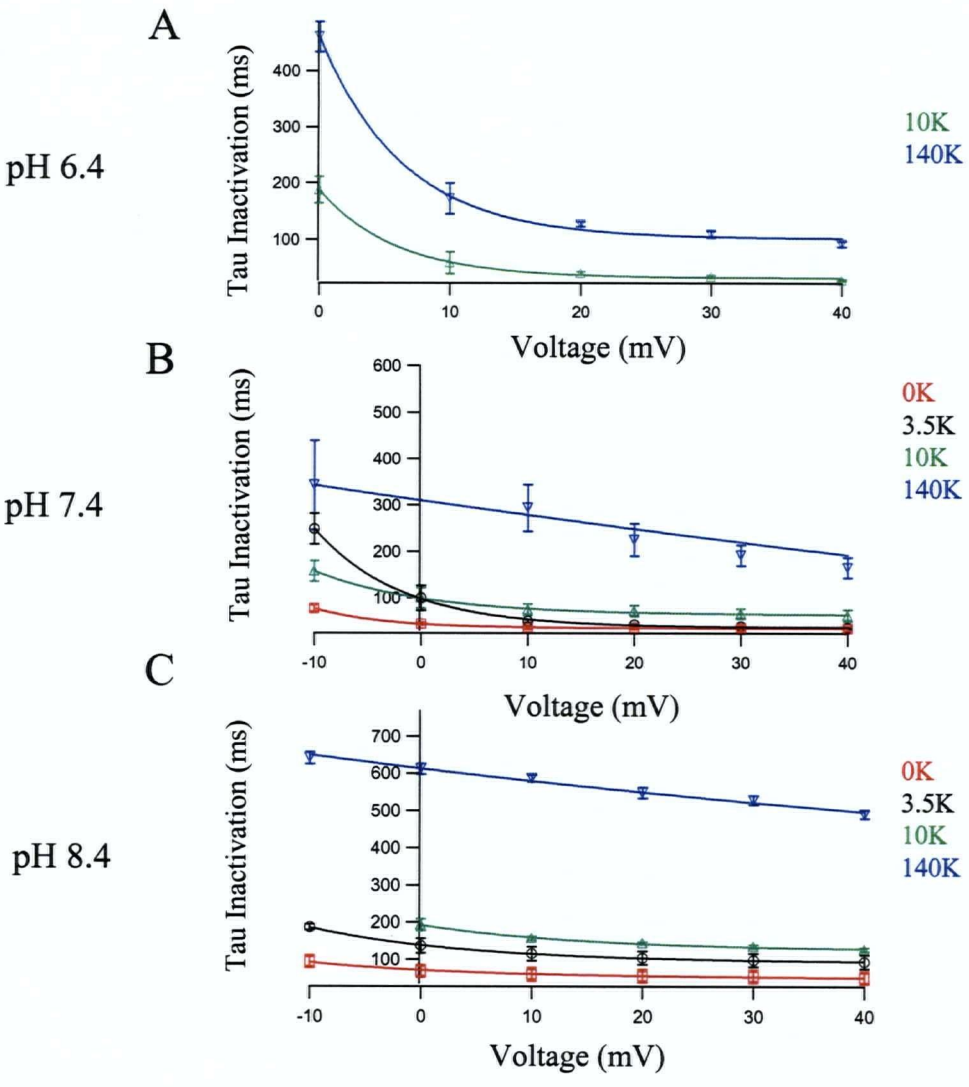


Figure 9 **140 mM $K^+_o$ significantly increases $\tau_{inact}$ in Kv1.5 H463R/R487H.**
**A, B and C** The decay phase of the current in Figures 7A, C and E was fit to a single exponential to approximate the time constant for inactivation. The $\tau_{inact}$ at pH 8.4 was fit to a single exponential from currents obtained with either a 2000ms pulse (140 mM $K^+_o$) or a 500 ms pulse (0 mM, 3.5 mM and 10 mM $K^+_o$). Analyzed data shows a clear $K^+_o$ and pH (slowest at pH 8.4) dependence to the time constant of inactivation. Increasing the extracellular $K^+$ concentration from 0 mM (red), to 3.5 mM (black), to 10 mM (green) caused a slight pH dependent increase of the $\tau_{inact}$. At pH 6.4, there was a voltage dependence to the time constant for inactivation between 10 mM and 140 mM $K^+_o$, however, as the pH was increased (8.4) the apparent voltage dependence of $\tau_{inact}$ disappeared. At pH 6.4, 7.4 and 8.4 the time constant for inactivation with 140 mM $K^+_o$ was significantly slower than with 0 mM, 3.5 mM or 10 mM $K^+_o$.

**$K^+_o$ and pH dependence of $\tau_{deact}$ of H463R/R487H**

Figures 10A, C and E show current traces at pH 6.4, 7.4 and 8.4 generated by pulsing from a holding potential of –80 mV to +50 mV for 15 ms, to fully activate the channels and to minimize inactivation, and then to voltages between –120 mV and -30 mV in 10 mV increments for 300 ms. The $\tau_{deact}$ was estimated by fitting the declining phase of the currents to a single exponential. The time constant for deactivation was only determined up to -30 mV because at more positive potentials there was a mixture of deactivation and inactivation in the tail current relaxations.

At pH 6.4 (Figure 10B), increasing the extracellular concentration of $K^+$ caused $\tau_{deact}$ to increase at voltages above –50 mV. The $\tau_{deact}$ at -30 mV in 10 mM and 140 mM $K^+_o$ was 4.5 ± 1.2 ms ($n$=3), 18.6 ± 1.8 ms ($n$=3), respectively. The $\tau_{deact}$ at -30 mV with 140 mM $K^+_o$ was significantly slower at pH 6.4.

At pH 7.4 (Figure 10D), $\tau_{deact}$ at +40 mV with 0 mM, 3.5 mM, 10 mM and 140 mM $K^+_o$ was 13.2 ± 1.5 ms ($n$=3), 10.1 ± 1.09 ms ($n$=5), 8.7 ± 0.5 ms ($n$=3), and 38.2 ± 5.2 ms ($n$=3), respectively. An extracellular $K^+$ of 140 mM at pH 7.4 significantly increased $\tau_{deact}$ in comparison to 0 mM, 3.5 mM, and 10 mM $K^+_o$ at -30 mV.

At pH 8.4 (Figure 10F), $K^+_o$ had a minimal effect with 0 mM, 3.5 mM and 10mM $K^+_o$. The $\tau_{deact}$ at -30 mV with an extracellular concentration of $K^+$ of 0 mM, 3.5 mM, 10 mM and 140 mM was 8.7 ± 1.8 ms ($n$=4), 14.0 ± 3.6 ms ($n$=3), 5.5 ± 1.2 ms ($n$=3), and 24.8 ± 3.3 ms ($n$=4), respectively. It was found with 140 mM $K^+_o$ at pH 8.4 there was a significant increase of $\tau_{deact}$ at -30 mV.

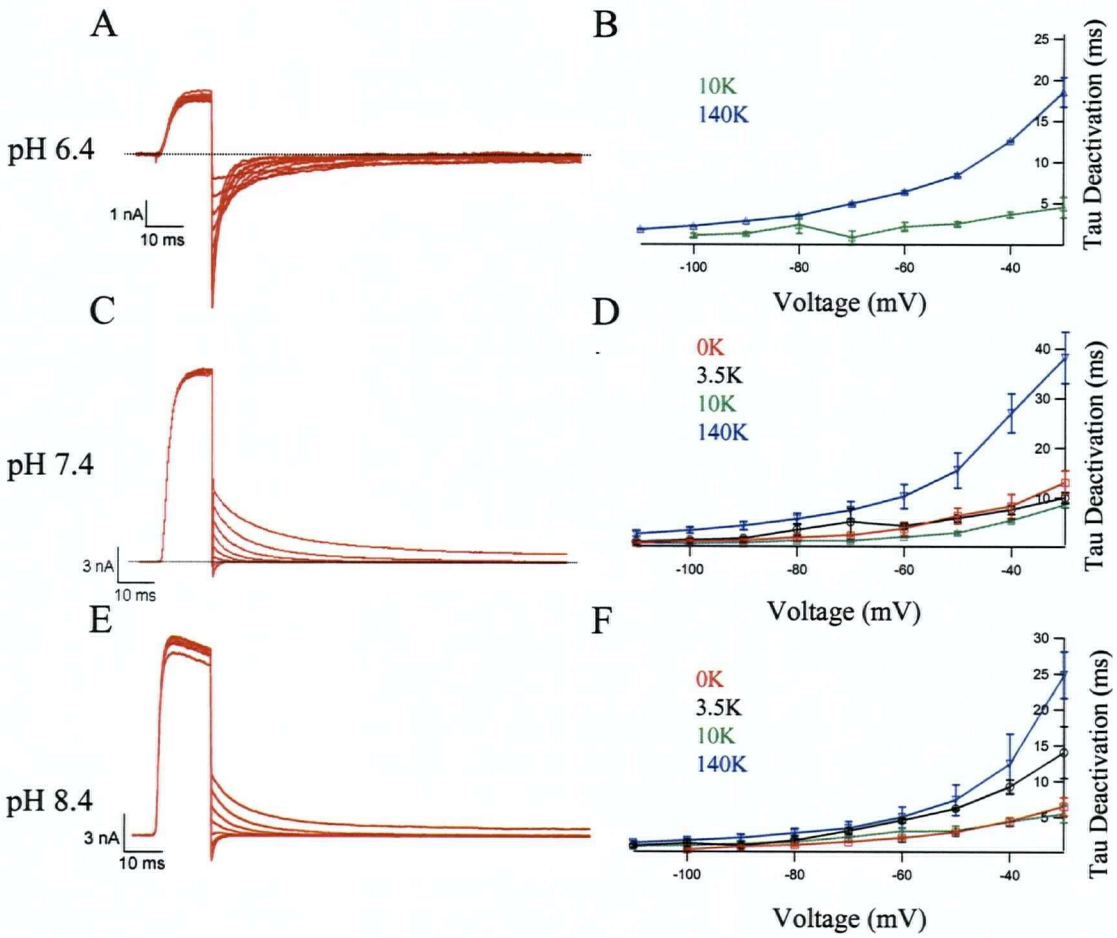


Figure 10 **The time constant for deactivation in Kv1.5 H463R/R487H is $K^+_o$, but not pH-dependent. A, C and E** Representative current traces at pH 6.4 (140 mM $K^+_o$), 7.4 (3.5 mM $K^+_o$), or 8.4 (10 mM $K^+_o$) were generated by stepping from a holding potential of –80 mV to +50 mV for 15 ms and then to a voltage between -120 and -30 mV for 300 ms. The decay phase of the current trace was fitted to a single exponential to approximate the time constant for deactivation. The $\tau_{deact}$ at $V_m > -30$ mV was not determined as there was a contamination of the rate of deactivation by inactivation. **B, D and F** Analyzed data shows a clear voltage and $K^+_o$ dependence to the $\tau_{deact}$. Extracellular concentrations 0 mM (red), 3.5 mM (black), 10 mM (green) and 140 mM (blue) $K^+_o$ were used to determine the $K^+_o$ dependence of the mutant. At pH 6.4, 7.4 and 8.4, 140 mM $K^+_o$ was found to significantly increase the time constant for deactivation at –30 mV.

**$K^+_o$ and pH Dependence of H463Q/R487H**

In Figure 11 the double mutant Kv1.5 H463Q/R487H was studied to further investigate the role that an electrically neutral charge at position 463 in the turret has on macroscopic current kinetics. In wild-type Kv1.5 at pH 7.4 the time constant for inactivation is ~1.3s at +40 mV, with 3.5 mM $K^+_o$ and not dependent on $K^+_o$, however, with extracellular acidification (pH 6.4) there is $K^+_o$ dependence and a reduction in the $\tau_{inact}$ (Kehl *et al.*, 2002). To this point (Figures 6-10) we have shown that a 'permanently' charged residue (H463R) at position 463 accelerates inactivation, and that 140 mM $K^+_o$ significantly increases the time constant for inactivation. In this next section, we mutated the residue at residue 463 to a glutamine (H463Q) with the expectation that it would increase the $\tau_{inact}$ and abolish the $K^+_o$ dependence.

Figures 11A and B show representative current traces at pH 7.4 and 6.4, respectively, with 3.5 mM $K^+_o$. Currents were generated by pulsing from a holding potential of –80 mV to a voltage between –40 and +40 mV for 2000 ms, followed by a repolarization to -70 mV for 200 ms. Analysis of the decay phase, which was fit to a single exponential, gave a $\tau_{inact}$ of ~1.3 s and ~2.3 s with 3.5 mM $K^+_o$ at pH 7.4 and 6.4, respectively. This result is in contrast to that of the H463R/R487H mutant in which the time constant for inactivation was 30-fold smaller (~35 ms) with 3.5 mM $K^+_o$ at pH 7.4. At pH 6.4 with 3.5 mM $K^+_o$, the outward currents in Kv1.5 H463R/R487H were very small (most of the channels were unavailable); however, with the H463Q/R487H mutant outward currents did not collapse. The results from this section suggest that an electrically neutral charge at position 463 slows inactivation, and stabilizes the open conformation at pH 6.4.

In Figure 11C, representative current traces at pH 6.4 and pH 7.4, 0 and 3.5 mM $K^+_o$, show the pH dependence of the H463Q/R487H currents on $I_{max}$. Currents were elicited by pulsing from a holding potential of -80 mV to +50 mV for 3000 ms and then repolarized to -50 mV for 200 ms. There was a small reduction in $I_{max}$ with both 0 mM and 3.5 mM $K^+_o$ at pH 6.4.

In Figure 11D the currents with 0 mM and 3.5 mM at pH 6.4 and 7.4 were normalized to compare the time constant for inactivation. At pH 7.4, 0 mM and 3.5 mM $K^+_o$, resemble wild-type Kv1.5 data in that there is no $K^+_o$ dependence to the $\tau_{inact}$ or current magnitude at +40 mV. At pH 6.4 in Kv1.5 H463Q/R487H, unlike wild-type Kv1.5, there are distinguishable currents with 0 mM $K^+_o$, that appear to inactivate over the same time course as 3.5 mM $K^+_o$. In the normalized traces, there is no significant difference in the rates of inactivation between 0 mM and 3.5 mM $K^+_o$ at pH 7.4, or 0 mM and 3.5 mM $K^+_o$ at pH 6.4.

These results suggest that neutralization of the charge at 463 increases $\tau_{inact}$, abolishes the $K^+_o$ dependence, and stabilizes the open conformation of Kv1.5 H463Q/R487H at pH 6.4. Unlike other Kv channels, there is no $K^+_o$ dependence to the time constant for inactivation of Kv1.5 H463Q/R487H at pH 6.4 or 7.4, suggesting that the $K^+_o$-dependence in wild-type Kv1.5 (3.5 mM vs. 140 mM $K^+_o$, at pH 6.4) is a result of the protonation state of H463. However, it is probably incorrect to suggest that a residue with an electrically neutral charge at position 463 is the only factor that is affecting the time course of inactivation and current decay. We were unable to express the single histidine mutation at residue 487 (R487H), so we can't conclusively say that a partially charged residue in the pore is not contributing to the observed effects.

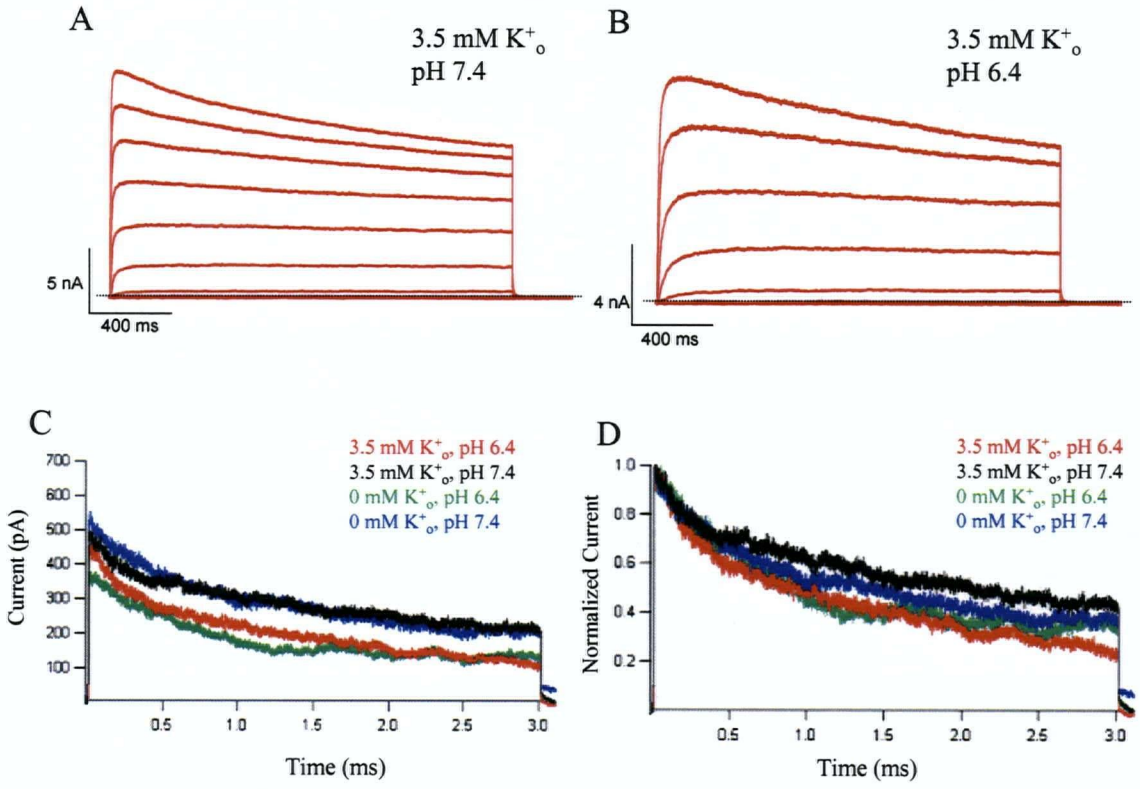


Figure 11 **The time constant for inactivation of Kv1.5 H463Q/R487H is pH (6.4 and 7.4) but not $K^+_o$ dependent. A and B**, Representative current traces from the same cell at pH 6.4 or 7.4 with 3.5 mM $K^+_o$ were generated by pulsing from a holding potential of –80 mV to +50 mV for 2000 ms followed by a repolarization to –70 mV for 200 ms. Mutation of the histidine residue at position 463 to a glutamine increased the $\tau_{inact}$ at pH 6.4 and 7.4 to 1.3s and 2.1s, respectively. The rates of inactivation were determined by fitting the current decay to a single exponential function. **C,** Representative traces at pH 6.4 and 7.4, with 0 mM and 3.5 mM $K^+_o$, show the currents generated by stepping from -80 mV to +50 mV for 3000 ms, and then repolarizing to -50 mV for 200 ms. From the traces it was determined that changing the $K^+_o$ did not significantly affect the reduction of $I_{max}$ at pH 6.4. **D**, Scaled currents at pH 6.4 and 7.4 (0 mM and 3.5 mM $K^+_o$) show the pH and $K^+_o$ dependence of $\tau_{inact}$. At pH 7.4 there was no significant difference in the time constant for inactivation between 0 mM and 3.5 mM $K^+_o$ at +40 mV. At pH 6.4, there was a decrease in the time constant for inactivation compared to pH 7.4 with 0 and 3.5 mM $K^+_o$ at +40 mV, however, there is no difference in the rate of inactivation between 0 mM and 3.5 mM $K^+_o$ at pH 6.4. This result is in sharp contrast to wild-type Kv1.5 in which there is an 80% reduction in the peak current at pH 6.4 with 0 mM $K^+_o$.

The results from the double mutant Kv1.5 H463R/R487H suggest that this mutant is both pH dependent and $K^+_o$ dependent. Elevation of the external concentration of $K^+$ (140 mM) significantly increases the $\tau_{inact}$ and $\tau_{deact}$, but does not affect activation. The questions arising from this section are: (1) How is increasing the extracellular concentration of $K^+$ affecting the time constant for deactivation and inactivation? (2) Why are the currents in 10 mM and 140 mM $K^+_o$ larger than with 3.5 mM $K^+_o$? (3) How is changing the pH altering the $K^+_o$ effect on the $V_{1/2}$, the slope factor and inactivation time constant?

Kv1.5 H463Q/R487H suggests that the charged residue at position 463 underlies the fast inactivating, and pH-dependent profile of the H463R/R487H mutant. This result is in support of results from Kv1.5 H463Q in which neutralization of the protonatable group at 463 prevented the acceleration of inactivation at pH 6.4.

## Discussion

### Part I: Permeation through Kv1.5 R487V

The first section of this thesis investigated a role of the charged residue (R487, *pKa* = 10.5) in the outer pore mouth of Kv1.5 in permeation. The first series of experiments (Figs 2-5) showed that neutralization of a charged residue to a valine (R487V) causes Kv1.5 channels to behave in an inwardly rectifying manner.

**Neutralization of R487 in Kv1.5 or K533 in Kv1.4 reduces current amplitude in symmetrical $K^+$ at positive voltages**

In Kv1.4 neutralization of K533 (*pKa* = 12.5), the structural analogue of R487 in Kv1.5, to a tyrosine (K533Y) causes the channel to have a non-linear *I-V* relationship (Ludewig *et al.*, 1993). At positive voltages, normalized currents through K533Y at +120 mV are approximately 2.5-fold smaller than the currents generated at –120 mV. In wild-type Kv1.5 and Kv1.4 there are some striking differences between the $K^+_o$ dependence and the residue at 487 in Kv1.5 (K533 in Kv1.4). In the absence of extracellular $K^+$ in Kv1.4 there is almost a complete loss of current at pH 7.4 (Pardo *et al.*, 1992). Through site-directed mutagenesis it was shown that replacement of the lysine residue at 533 (K533) with a neutral residue makes Kv1.4 insensitive to changes in $K^+_o$ (Pardo *et al.*, 1992). In Kv1.3 the analogous residue to R487 in Kv1.5 is a histidine at position 404 (H404). At pH 7.4 this channel does not show sensitivity to extracellular $K^+$; however, when the pH is decreased to 6.4, the protonation state of the histidine at position 404 changes and Kv1.3 current collapses with 0 mM $K^+_o$ (Jager *et al.*, 1998). These results suggest that the presence of a charged residue at the outer pore mouth makes both the time constant for inactivation and $I_{max}$ sensitive to $K^+_o$.

In Kv1.5, the arginine at position 487 is assumed to be charged, however, in 0 mM $K^+_o$ the channel does not collapse, in sharp contrast to Kv1.4 and Kv1.3 channels (Jager & Grissmer, 2001; Kehl et *al* 2002). In an effort to further investigate the structure-function relationship between Kv1.4, Kv1.3 and Kv1.5, we mutated the residue analogous to Kv1.4 K533 in Kv1.5 (R487) to determine if the open channel *I-V* relationship would replicate that of Kv1.4 K533Y.

In symmetrical $K^+$, wild-type Kv1.5 has a linear *I-V* relationship from –120 to +140 mV (Figure 2B). Neutralization of the charge on the residue at position 487 (R487V) caused the *I-V* relationship to become non-linear (Figure 3C). Initially, experiments were performed with a free intracellular $Ca^{2+}$ concentration of 50 nM. At voltages above +50 mV there was a steeply voltage dependent block of outward currents by $Ca^{2+}$ ions blocking the pore (Figure 3C- black trace). This effect has been shown in macroscopic Kv1.5 currents (Kwan *et al.*, 2004b), inwardly rectifying Kv channels (Matsuda *et al.*, 1987) and Kv1.4 (Ludewig *et al.*, 1993) channels at depolarized potentials greater than +50 mV. To investigate the behavior of currents at voltages greater than +50 mV subsequent experiments were performed with no added $Mg^{2+}$ or $Ca^{2+}$ ions in the intracellular solution. In symmetrical $K^+$, with no added $Ca^{2+}_i$, the normalized current was 2.17 fold greater at -120 mV than +120 mV (Figure 3C- red trace). This result was similar to the reduction seen in Kv1.4 over a similar voltage range (Ludewig *et al.*, 1993).

Large conductance $K^+$ (BK) channels have a single channel conductance of ~300pS in symmetrical $K^+$, which is approximately 6-fold larger than the conductance of most Kv1 channels (Latorre *et al.*, 1989). In BK channels there are 2 negatively charged

residues from each α- subunit (8 in total) that are positioned at the intracellular entrance to the pore (Mackinnon *et al.*, 1989; Doyle *et al.*, 1998; Nimigean *et al.*, 2003; Brelidze *et al.*, 2003). It was hypothesized that these charged residues, in the homotetrameric assembly, form a ring of negative charges that concentrate $K^+$ ions at the intracellular entrance to the pore. Mutation of these residues, E321N and E324N, significantly reduces the outward current through BK channels, supporting the hypothesis that neutralization of a charged residue affects the permeation of $K^+$ at the outer pore mouth (Doyle *et al.*, 1998; Brelidze *et al.*, 2003; Nimigean *et al.*, 2003). Neutralization, by mutation, of charged residues near the pore mouth have yielded similar results in Kv2.1 (Consiglio *et al.*, 2003), $Na_v$ channels (Li *et al.*, 2000), AChR's (Imoto *et al.*, 1988) and CFTR channels (Smith *et al.*, 2001). Similar to the charged ring formed by E321 and E324 in BK channels at the intracellular vestibule of the channel, it is hypothesized that E292 forms a ring of negative charge at the extracellular vestibule of BK channels. Neutralization of this residue causes a large reduction of the normalized inward current magnitude through BK channels (Haug *et al.*, 2004).

These results suggest that the change in the *I-V* relationship of Kv1.5 R487V may result from a change in the 'effective' $[K^+]$ at the outer pore mouth.

**The current magnitude and *I-V* relationship is pH insensitive in Kv1.5 R487V**

It has previously been shown that wild-type Kv1.5 is pH sensitive, with acidification reducing the magnitude of outward currents in 0 mM and 3.5 mM $K^+_o$ (Steidl & Yool, 1999; Jager & Grissmer, 2001; Kehl *et al.*, 2002). Mutation of the arginine at position 487 to a valine (R487V) dramatically reduces the sensitivity of Kv1.5 to extracellular pH (Kehl *et al.*, 2002). To determine if the protonation state of the

histidine at position 463 affected permeation through Kv1.5 R487V channels we changed the $pH_o$ with the intent of protonating the histidine at position 463. At pH 6.4, 7.4 and 8.4 there was no change in the amplitude or kinetics of Kv1.5 R487V with symmetrical $K^+$ (Figure 4A). This result was also evident in the *I-V* relationship as the normalized currents at +120 mV were ~2.17-fold smaller the inward currents at –120 mV (Figure 3B), analogous to pH 7.4 (Figures 3C).

It has been suggested that in the open conformation residues 487 and 463 in wild-type Kv1.5 are located close enough that they may be able to influence the *pKa* (protonation state) of one another (Jager & Grissmer, 2001). However, it was been shown that the *pKa* for Kv1.5 H463 (Kehl *et al.*, 2002) and K425H in *Shaker* (Perez-Cornejo *et al.*, 1999) is ~6.2, the normal *pKa* value for a free histidine side group. This suggests that the protonation state of the histidine was not influenced by the residue at position 487, and thus mutation to a valine will not alter the protonation state of Kv1.5 H463.

The result from Figure 4B suggests that the rate at which ions are able to leave the pore is not modulated by having a charged residue in the turret and that the changes in the outer mouth that are responsible for the non-linear *I-V* relationship in Kv1.5 R487V are not through an interaction between H463 and the pore.

**Changes in the outer vestibule associated with Kv1.5 R487V**

The rate at which ions are able to permeate an open channel is a complex process that involves many physical and chemical interactions. The generation of a computer model is an attempt to create a dynamic view of the interactions that are occurring at the ionic level as ions pass through the pore. Models of ion permeation through $Ca^{2+}$ channels (Almers & McCleskey, 1984; Hess & Tsien, 1984) and Kv1.4 (Ludewig *et al.*,

1993) have previously been shown to accurately model experimental data through alterations in the free energy barriers of the permeation pathway by a Eyring model. In our Eyring-rate model a symmetrical pore with 2 binding sites was used to simulate the permeation pathway through Kv1.5 and Kv1.5 R487V (Figure 5A). The free energy values used for the model were similar to those used in the Kv1.4 model (Ludewig *et al.*, 1993) (Figure 5A) and from the knowledge that the single channel current through wild-type Kv1.5 at +100 mV is ~1.5pA (data not shown) (Kwan *et al.*, 2004a). Figures 5B and C show both the experimental and modeled data, respectively, through Kv1.5 and Kv1.5 R487V channels in symmetrical $K^+_o$.

In Kv1.5 R487V, the modeled data is able to replicate the trends observed in the experimental data. In wild-type Kv1.5 and the modeled data with symmetrical 140 mM $K^+$ there was a linear *I-V* relationship. However, in Kv1.5 R487V neutralization of a positive residue in the outer pore at position 487 caused a reduction in the normalized outward current, possibly through a change at the outer pore mouth. To test this hypothesis in the model, the external energy barrier and external $K^+$ binding site were increased and decreased, respectively, by 1 *RT* unit to account for the changes at the outer vestibule. In the modeled data and R487V there is a ~2-fold reduction in the current at +100 mV when compared to the normalized current at –100 mV. In addition to accurately representing the non-linear *I-V* relationship, the model is able to accurately show the changes that occur at negative potentials. An increase in the external energy barrier, or decrease of the external binding site, will not only affect the rate at which ions can leave the external vestibule but it will also affect the rate at which ions can make the transition between the external and internal sites. The change in the *I-V* relationship was most

evident at less negative voltages (-80 to –30 mV) where ions will experience less of the electric field reducing the normalized inward current.

The experimental results and modeled data of the permeation pathway through Kv1.5 R487V suggest that a change is occurring at the outer vestibule with neutralization of the charge at position 487. An elevation of the external energy barrier (Figure 5A) may be interpreted to account for a reduction in the electrostatic repulsion that occurs when a $K^+$ ion is leaving the outer site. A positively charged ion that enters the outer vestibule will be electrostatically repelled from the mouth of the pore into the bulk solution. Mutation of the residue at position 487 to a valine decreases the electrostatic forces that are acting to clear $K^+$ ions from the outer vestibule, decreasing outward and inward ion flux. A reduction of the external binding site suggests that $K^+$ ions have a higher affinity with neutralization of R487 (R487V). This result may indicate that having a positively charged residue at the external mouth acts to decreasae the dwell time, or affinity, of a $K^+$ ion in the permeation pathway. If the charge on 487 is removed, $K^+$ ions will have a longer dwell time, possibly through a conformation change, and the outward flux of $K^+$ ions will be reduced. We were unfortunately unable to express R487E, however, this mutant may have allowed us to provide further insight into the mechanism that is changing the permeation pathway of Kv1.5 R487V through a mechanism of electrostatic attraction.

There are some shortcomings to the Eyring-model that we have used to test the non-linear *I-V* relationship of Kv1.5 R487V. In our Eyring model we have used a 2-site model to approximate the behavior of $K^+$ ions as they permeate through the pore. Crystallization of a Kv channel pore has shown that there are 4 $K^+$ binding sites in the

pore, and not the 2 that we have used to approximate our data (Zhou *et al.*, 2001; Jiang *et al*, 2002). In the crystal structure of the Kv pore it has been shown there can never be more than 2 sites in the permeation pathway occupied at the same time. Therefore, although incorrect, we have used a less technical approach by only having 2 binding sites to approximate the behavior of the 4-site Kv pore. We have accepted this model because it is able to accurately approximate the experimental data.

In addition we have also not included a repulsive factor in our Eyring model of the permeation pathway through Kv1.5. It has been shown in $Ca^{2+}$ channels that a repulsive factor is required to replicate the single channel currents seen in the wild-type channels (Almers & McCleskey, 1984). Additionally, data from $Na^+$ permeation in squid giant axons has been replicated using an Eyring-rate model with no repulsive factor (Begenisich & Cahalan, 1980a; Begenisich & Cahalan, 1980b). In our model, changing the free energy profiles approximated the single channel current of Kv1.5 with 140 mM $K^+_o$ and therefore we have not added a repulsive factor (data not shown).

In conclusion, the reduction of the normalized current at positive voltages in Kv1.5 R487V is a result of a change in the electrostatic properties of the outer vestibule. A positively charged residue in the external mouth of the channel (R487) will create an electrostatic potential that will repel $K^+$ ions into the bulk solution. Mutation of R487V to a valine significantly reduces the magnitude of the normalized outward current and decreases the rate of permeation through Kv1.5 channels.

**Part II: $pH_o$ and $K^+_o$ dependence of Kv1.5 H463R/R487H**

It has previously been shown in wild-type Kv1.5 that extracellular acidification from pH 7.4 to as low as pH 5.5 decreases the magnitude of outward currents ($I_{max}$) and

decreases the time constant for inactivation (Jager & Grissmer, 2001; Kehl *et al.*, 2002). In Kv1.5 there is a protonatable histidine group in the turret region at position 463 ($pKa$ = 6.2, although the apparent $pKa$ is $K^+_o$ sensitive). It is thought that with extracellular acidification H463 becomes protonated, changing channel availability and $\tau_{inact}$. In part II of this thesis we mutated the histidine at position 463 in Kv1.5 to a positively charged arginine group ($pKa$ = 10.5) to investigate the effect of having a 'permanently' charged group at this site over a wide pH range on channel function (Figure 12). In addition to investigating the role of a charged residue at position 463, we wanted to determine how a protonatable group at 487 would alter channel functioning (Figure 12). It has previously been shown that Kv1.5 R487H is not sensitive to changes of $[K^+_o]$ at pH 7.4, however, with extracellular acidification the current collapses with 0 mM $K^+_o$ and the time constant for inactivation with 3.5 mM $K^+_o$ is decreased (Jager & Grissmer, 2001). However, in Kv1.5 R487H it is unclear if the changes to $\tau_{inact}$ and channel availability are a result of a change in the protonation state of the histidine at position 463 or 487. It is our hypothesis that Kv1.5 H463R/R487H will decrease the time course for inactivation in comparison to wild-type Kv1.5 and cause the channel to behave at pH 7.4 and 8.4 like wild-type channels at pH 6.4 ($K^+_o$ dependence to the $\tau_{inact}$ and channel availability).

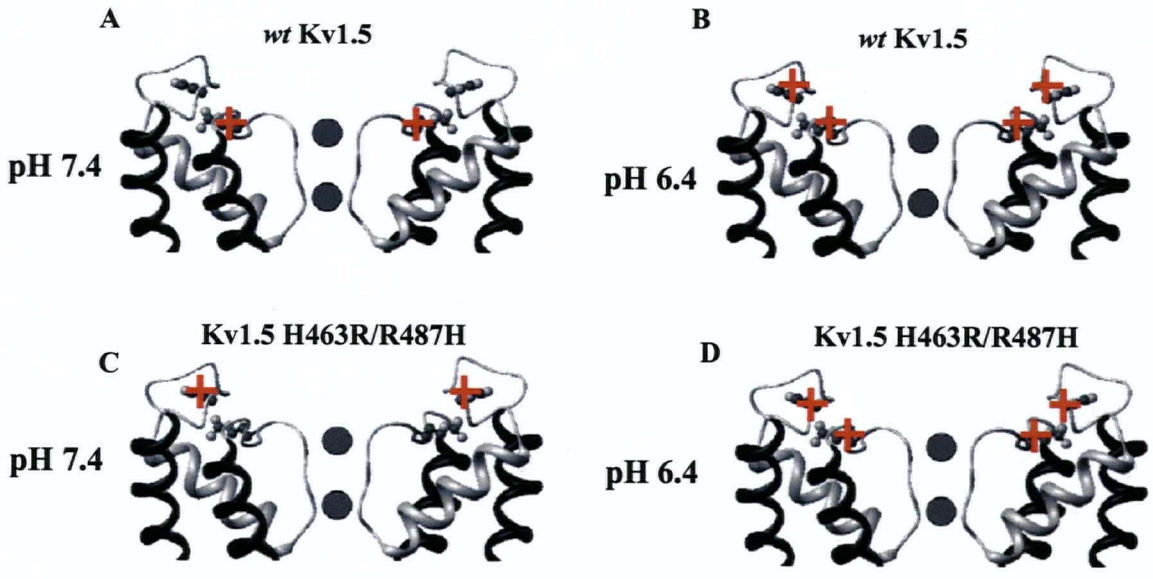


Modified from (Kehl *et al.*, 2002)

Figure 12 **The 'relative' charge of positions 463 and 487 at pH 6.4 and 7.4 in wild-type Kv1.5 and Kv1.5 H463R/R487H. A**, In wild-type Kv1.5 at pH 7.4 there is a 'permanently' charged residue in the outer pore mouth at position 487. **B**, Extracellular acidification (pH 6.4) changes the protonation state of the histidine residue at position 463 resulting in a second positive charge in wild-type Kv1.5, one charge is in the outer pore mouth while a second is located in the turret. **C**, In Kv1.5 H463R/R487H there is a 'permanently' charged residue in the turret region of Kv1.5. **D**, At pH 6.4 the protonation state of the histidine residue in the outer pore mouth changes and a positive charge is now present. The aim of this experiment was to investigate the effect on channel function of a 'permanently' charged residue in the turret of Kv1.5 and a protonatable residue in the outer pore mouth.

Experimental findings in other Kv channels have shown that despite structural and sequence similarities there are significant discrepancies in the processes of inactivation and $K^+_o$ sensitivity. In Kv1.3 and Kv1.4 a charged residue at the outer pore mouth, H404 and K533, respectively, makes the channels sensitive to changes in $K^+_o$; however, this $K^+_o$-dependence is not seen in Kv1.5 (R487 in Kv1.5) even though there is a charged residue in the analogous position. Characterization of Kv1.5 H463R/R487H

will provide further insight into the role of 2 previously implicated residues, H463 and R487, in channel inactivation and $K^+_o$ sensitivity. Therefore, in the second section of this thesis (Figures 6-10) the effect of pH and $K^+_o$ on the half-activation voltage ($V_{1/2}$), slope factor ($k$), and time constants for inactivation, activation and deactivation of Kv1.5 H463R/R487H were determined. From the results in this second section there are 2 common trends: (1) 140 mM $K^+_o$ increases the time course for channel inactivation at all pH values, and, (2) The maximal outward current at +40 mV is pH dependent.

**The time constant for inactivation in H463R/R487H is significantly faster than wild-type Kv1.5**

At pH 7.4 with 3.5 mM $K^+_o$ the time constant for inactivation at +40 mV in H463R/R487H (~35 ms) is approximately 30-fold smaller than that of wild-type Kv1.5 (~1.3 s) at +40 mV when fit to a single exponential function (Kehl *et al.*, 2002). It has previously been shown that mutation of the histidine at position 463 to a glutamate, lysine, arginine, glycine or alanine accelerates the time course for inactivation in Kv1.5 at least 5-fold (Kehl *et al.*, 2002; Eduljee *et al.*, 2004). In addition to accelerating inactivation, mutation of the histidine at position 463 to an arginine (H463R) in Kv1.5 shifts the $K_D$ for channel availability to the right and increases the time constant for recovery from inactivation (Eduljee *et al.*, 2004). However, mutation of H463 to a glutamine (H463Q) had a $\tau_{inact}$ similar to that of wild-type Kv1.5 and the time constant in Kv1.5 H463Q was not pH insensitive, unlike wild-type Kv1.5 (Kehl *et al.*, 2002). In *Shaker* channels mutation of the phenylalanine at position 425 to a histidine (F425), analogous to H463 in Kv1.5, decreased the $\tau_{inact}$, and made it sensitive to changes in $pH_o$ (Perez-Cornejo, 1999). Therefore, it can be inferred, from data in *Shaker* and Kv1.5

channels, that the size and charge of the residue at position 463 in Kv1.5 has a significant effect on the time constant for inactivation.

It has been shown in other Kv1 channels that a charged residue at the position analogous to 487 in Kv1.5 can change the inactivation time course and $K^+_o$ sensitivity of the channel. In *Shaker* Kv channels it has previously been shown that mutation of the residue at position 449 affects $\tau_{inact}$ and makes the channel sensitive to changes in $K^+_o$ (Lopez-Barneo *et al.*, 1993; Molina *et al.*, 1998). In Kv1.4, the analogous residue to R487 in Kv1.5 is K533. In Kv1.4 the rate of inactivation, and peak current amplitude is $K^+_o$ sensitive at pH 7.4 (Pardo *et al.*, 1992); whereas, this effect is not seen in Kv1.5 (Jager *et al.*, 1998; Kehl *et al.*, 2002). In Kv1.3 channels there is a protonatable histidine group at position H404, analogous to R487 in Kv1.5, and it has been shown that extracellular acidification causes the channel to inactivate faster and show $K^+_o$ sensitivity (Jager *et al.*, 1998). In Kv1.3, the analogous residue to H463 in Kv1.5 is a glycine, which is not protonatable and therefore not a contributing factor to the changes in channel kinetics in Kv1.3 (unlike Kv1.5).

Mutation of R487 in Kv1.5 to a valine (V) or tyrosine (Y) does not affect the time constant for inactivation of Kv1.5 (Fedida *et al.*, 1999). This result indicates that a charged residue at this position is not required for the channel to inactivate with wild-type kinetics. It has previously been reported in Kv1.5 R487H that the $\tau_{inact}$ is similar to that of wild-type Kv1.5 at pH 7.4 and that external acidification both accelerates the time course for inactivation in 4.5mM $K^+_o$ and collapses the current in 0 mM $K^+_o$ (Jager & Grissmer, 2001). This result suggests that the histidine at position 487 is not protonated at pH 7.4 and thus not $K^+_o$ sensitive. However, it is difficult to accept that current collapse and $K^+_o$

sensitivity in Kv1.5 R487H at pH 6.4 was a only a result of a change in the protonation state of R487H as there will also be a charge at position 463 (protonated histidine), which is known to confer $K^+_o$ sensitivity (Eduljee *et al.*, 2004).

The turret region of *Shaker* channels (E418 to D431) (E456 to P468 in Kv1.5) has previously been shown to affect the stability of the activated state (Loots & Isacoff, 1998; Larsson & Elinder, 2000). It was reported that a highly conserved glutamate residue in Kv channels, E418 in *Shaker,* (E456 in Kv1.5) was important for the stability of the open conformation of the slow inactivation gate in *Shaker* channels. Neutralization of the acidic residue at position 418 (E418C) increased the rate of inactivation approximately 40-fold, slowed the rate at which the channel was able to recover from inactivation and decreased the functional expression of the channel by ~90% (Larsson & Elinder, 2000). In Kv1.5, mutation of E456 results in a mutant that is not at the cell surface (C. Eduljee and SJ Kehl, unpublished data). In *Shaker,* the selectivity filter (TXGYG) is hypothesized to be held in place by W434 and W435 (from adjacent subunits), which form hydrogen bonds with Y445 (G**Y**G of the selectivity filter) and are stabilized by a hydrogen bond formed between E418 and G452 (in the P-S6 linker). When this hydrogen bond (E418 to G452) in *Shaker* is broken, the outer pore (448-452) can undergo a conformational change and enter the inactivated state (Loots & Isacoff, 1998; Larsson & Elinder, 2000). Therefore, I propose that a positive charge at position 463 in Kv1.5 might induce a conformational change (through an electrostatic interaction with E456 or D458) in the turret that decreases the probability of an interaction between E456 and either G492/G493. Destabilization of the open conformation would result in a smaller $\tau_{inact}$ and a slower rate of recovery from inactivation. This hypothesis would support the data for

H463R/R487H in which the time constant for inactivation is ~30-fold smaller at pH 7.4 with 3.5 mM $K^+_o$ (35 ms) than wild-type Kv1.5 (1.3 s), and recovery from inactivation is ~25-fold slower (2 s to 50 s) (data not shown) that with wild-type Kv1.5 channels at pH 7.4 with 3.5 mM $K^+_o$ (Figure 9B).

This hypothesis was also supported by the double mutant Kv1.5 H463Q/R487H in which neutralization of the charge at position 463 increased the time constant for inactivation and sped the rate of recovery from inactivation at pH 7.4 with 3.5 mM $K^+_o$ (1.3 s and 2 s, respectively) (Figure 11A) in comparison to the values for Kv1.5 H463R/R487H (previous paragraph). The time constant for inactivation in Kv1.5 H463Q/R487H was $K^+_o$ and pH insensitive suggesting that a charge at position 463 in Kv1.5 was an important determinant of these characteristics. This result suggests that neutralization of the charge at position 463, as it is the only altered variable, can stabilize Kv1.5 in the open conformation by allowing the turret and the pore to remain in a stable interaction that does not allow the pore to collapse.

A possible experiment to further test this hypothesis would be to decrease the ionic composition of the bulk solutions. If destabilization of the open conformation of the inactivated state occurs through an electrostatic interaction between E456 or D458 (an acidic residue in the turret of wild-type Kv1.5) and H463R, reducing the ionic composition of the solutions would further enhance this effect. If so, the time constant for inactivation would be smaller and there would be an increased sensitivity to $K^+_o$, and the $K_D$ for channel availability would be further shifted to higher $K^+_o$ concentrations.

There are some experimental findings that disagree with the hypothesis that a destabilization of the open of conformation occurs through an electrostatic interaction

between H463R and E456/E458 in the turret of Kv1.5. In Kv1.5, mutation of H463 to glycine and modification of a cysteine residue at position 462 (T462C) by propyl-methanethiosulfate (P-MTS) accelerates the rate of inactivation of Kv1.5 (Eduljee *et al.*, 2004; D. Chiang and S. Kehl, unpublished data). Mutation of H463 to a glycine (H463G) might be accelerating the rate of inactivation because a small uncharged residue at this position changes the conformation of the turret and does not permit an interaction between E456/D458 and G492. External modification of T462C by P-MTS may not permit the turret to undergo its complete conformational change with activation (locked in place by a large external group), inhibiting an interaction between the turret and pore regions of the channel, encouraging the inactivated state. In both of these instances acceleration of the rate of inactivation is not occurring through an electrostatic interaction but rather a conformational change of the turret. Therefore, although for different reasons, the result is consistent with the suggestion that changing the conformation of the turret accelerates entry into the destabilized inactivated state.

At pH 6.4, the accelerated time course of inactivation in 10 mM and 140 mM $K^+_o$ (2-fold faster than Kv1.5 H463R/R487H at pH 7.4) suggests that charged residues at 463 and 487 further destabilize the inactivated state and cause the channel to rapidly inactivate with depolarization. An elevated concentration of $K^+_o$ (140 mM) stabilized the open channel conformation by occupying the outer $K^+$ site, which in turn decreased the probability that the outer pore would collapse at pH 6.4. In 0 mM and 3.5 mM $K^+_o$ there is a low probability that the outer $K^+_o$ binding site is occupied causing the channel to collapse in either of these concentrations possibly through a closed-state inactivation

process (Lopez-Barneo *et al.*, 1993; Kehl *et al.*, 2002) for which there is some evidence from single channel recordings (Kwan DC, Fedida F and Kehl SJ, in revision).

**At pH 6.4 there is a collapse of current in 0 mM and 3.5 mM $K^+_o$ in Kv1.5 H463R/R487H**

At pH 6.4 there was a collapse of current in 0 mM and 3.5 mM; however, with 10 mM $K^+_o$ there were discernable currents. In Kv1.5 it has been shown that with 0 mM $K^+_o$ at pH 6.4 the maximal conductance is reduced by 85% in comparison to pH 7.4 (Kehl *et al.*, 2002) and that neutralization of the residues at position 463 (H463Q) or position 487 (R487V) reduce the effect of external pH on $I_{max}$ (Kehl *et al.*, 2002). In Kv1.5 the mechanism of proton inhibition of current is thought to occur through an outer pore inactivation process since elevation of $K^+_o$ decreases the effect of external acidification on $g_{max}$. In Kv1.5 H463R/R487H at pH 6.4, assuming there is no change in the *pKa* of H or R, there is a 'permanently' charged residue at position 463 (*pKa* = 10.5) and a partially protonated residue at position 487 (*pKa* = 6.2) which collapses current in 0 mM as well as 3.5 mM $K^+_o$ (Figure 6B). In Kv1.5 H463Q/R487H extracellular acidification (pH 6.4) did not collapse outward currents at +50 mV, but reduced $I_{max}$ by ~20% compared to pH 7.4, suggesting that an electrically neutral residue at position 463 in Kv1.5 stabilizes the open conformation and maintains channel availability with low $K^+_o$ (0 mM and 3.5 mM).

These results suggest that a positively charged residue at 463, and not 487, has the greater influence on the rate of inactivation and current collapse at pH 6.4. The $K^+_o$ dependence at pH 6.4 suggests that elevation of $K^+_o$ acts in a 'foot-in-the-door' manner to slow the rate at which the bond between E456 and G492 is destabilized, in a similar method by which $K^+_o$ can stabilize the E418C mutation in *Shaker* (Ortega-Saenz *et al.*, 2000). This result, along with data obtained with 10 mM and 140 mM $K^+_o$, supports the

notion that the $H^+_o$ effect on Kv1.5 H463R/R487H is mediated through outer pore inactivation as higher concentrations of $K^+_o$ generate appreciable currents.

Unlike Kv1.5 H463R/R487H at pH 6.4 with 3.5 mM $K^+_o$, wild-type Kv1.5 has discernable currents with 3.5 mM $K^+_o$ during a depolarizing pulse. I propose that this result occurs because the histidine at position 463 is not fully protonated and some channels will remain in the uncharged state (wild-type inactivation kinetics/stable E456-G492/G493 interaction), and maintain their ability to pass current at pH 6.4. Therefore, the collapse of current at pH 6.4 with 0 mM and 3.5 mM $K^+_o$ results from a positively charged arginine residue at position 463 which destabilizes the open conformation.

**Elevation of extracellular $K^+_o$ slows deactivation but does not affect the rate of activation in Kv1.5 H463R/R487H**

In the previous section it was shown that elevation of $K^+_o$ (140 mM) rescues channels from collapsing at pH 6.4 in Kv1.5 H463R/R487H. An elevation of extracellular $K^+$ increases the probability that the outer $K^+$ binding site is occupied and reduces the probability that the selectivity filter can collapse (possibly through a destabilization of the interaction between W434/W435 and Y446 in *Shaker* (Fedida *et al.*, 1999; Larsson & Elinder, 2000; Jager & Grissmer, 2001; Kehl *et al.*, 2002).

In *Shaker* and hERG $K^+$ channels there is no effect of elevating extracellular $K^+$ on the kinetics of activation or deactivation (Zagotta *et al.*, 1994a; Wang *et al.*, 1997). In Kv 4.3 (Wang *et al.*, 2004) and delayed rectifier currents (Swenson & Armstrong, 1981) increasing the $[K^+_o]$ (140 mM) has been shown to increase the time constant for deactivation by increasing the occupancy of a site within the pore (Matteson & Swenson, 1986). This result suggests that the dissociation of $K^+$ from its external binding site occurs rapidly at low $K^+_o$, and that a high $K^+_o$ (140 mM) is required to observe a change

in deactivation kinetics (Wang *et al.*, 2004). In Kv1.5 H463R/R487H there was an increase in the time constant for deactivation in 140 mM $K^+_o$ because there was a high probability that a site in the pore of Kv1.5 would be occupied, possibly through a 'foot-in-the-door' model.

The time constant for activation in Kv1.5 H463R/R487H was not affected by changing the $K^+_o$ or changing the pH. This result suggests that the change in the time constants for inactivation and deactivation in Kv1.5 H463R/R487H occurs after movement of the S4 segment. This is in agreement with previous literature that has shown gating charge currents ($I_g$) in wild-type Kv1.5 are not affected by extracellular acidification (pH 6.4) (Kehl *et al.*, 2002). The process of activation appears to be unaffected in Kv1.5 H463R/R487H; however, gating current analysis would have to be completed to accurately say there are no changes in the kinetics of the 'on' gating charge.

**Increasing the extracellular pH shifts the $V_{1/2}$**

It has previously been shown that external acidification causes a rightward shift in the $V_{1/2}$ of the activation curve of Kv1.5 (Steidl & Yool, 1999; Kehl *et al.*, 2002; Trapani & Korn, 2003). Although mutation of the histidine at position 463 to a glutamine (H463Q) decreases the $pH_o$-sensitivity of the $g_{max}$ of Kv1.5, it does not affect the pH-induced shift of the $V_{1/2}$ suggesting that there are 2 distinct areas where protons act. One of these regions is more than likely H463, as mutation of this residue decreases the pH sensitivity of the $g_{max}$ of Kv1.5, and the second area of action is probably through a surface charge effect at an unidentified residue that affects the $V_{1/2}$ (Kehl *et al.*, 2002).

In Kv1.5 H463R/R487H, extracellular acidification from pH 7.4 to 6.4 results in no significant change in either the slope factor for activation ($k$) or the half-activation

voltage ($V_{1/2}$) with 10 mM or 140 mM $K^+_o$ (Figure 7B and D). This result suggests that either H463R or R487H has removed the pH sensitivity as there is no depolarizing shift, as seen in wild-type Kv1.5, with extracellular acidification (Kehl *et al.*, 2002). A possible explanation for this observation is that mutation of position 463 in Kv1.5 to a 'permanently' charged residue, neutralized the negative charge at D458, and reduced the surface charge that the channel would normally be affected by to cause the shift in the $V_{1/2}$.

When the pH was increased from 7.4 to 8.4 there was no significant change in the $V_{1/2}$ or $k$ for 0 mM, 3.5 mM or 10 mM $K^+_o$; however, there was a significant shift in the $V_{1/2}$ and a 2-fold reduction in the slope factor with 140 mM $K^+_o$. The change in the slope factor may result from an increase in the rate constant for the final transition into the open state. It has previously been shown in a model with *Shaker* channels that a change in the $V_{1/2}$ and the slope factor may be accounted for by a change in the rate constant for the final transition to the open state, the magnitude of the 'on' and 'off' gating charge currents, or a de-stabilization of the open state (Smith-Maxwell *et al.*, 1998). The results in Figures 7D and F suggest that at pH 7.4 (in comparison to pH 8.4), the shift of the $V_{1/2}$ to the right and the reduction of the voltage dependence of channel opening can be accounted for by a slower transition to the open conformation from the final closed state.

**$I_{max}$ is $pH_o$ and $K^+_o$ dependent in Kv1.5 H463R/R487H**

From Figures 6A, C and E it is evident that pH and $K^+_o$ (by antagonizing the effect of extracellular protons and stabilizing the open conformation) have significant effects on the open probability of Kv1.5 H463R/R487H. At pH 6.4, there were no discernable currents with 0 mM or 3.5 mM $K^+_o$ and a progressive increase in $I_{max}$ with 10

mM and 140 mM $K^+_o$ (Figure 6A), despite the reduction in driving force. It has previously been suggested that with low $K^+_o$ external acidification causes the channels to become unavailable perhaps because of a closed state inactivation process, involving an outer pore mechanism (Lopez-Barneo *et al.*, 1993; Kehl *et al.*, 2002; Trapani & Korn, 2003). However, in Kv1.5 H463R/R487H there is virtually a complete collapse of the current at both 0 mM and 3.5 mM $K^+_o$. This result suggests that the $K_D$ for the $K^+_o$-dependence of channel availability is shifted to the right, and that a higher concentration of $K^+$ is required to stabilize the pore. In wild-type Kv1.5 (at pH 6.4) and Kv1.5 H463G (a rapidly inactivating mutant) the $K_D$ for the effect of $K^+_o$ on channel availability is ~1 mM. This result may suggest that in Kv1.5 H463R/R487H there is a conformational change in the structure/size of the external pore, shifting the $K^+_o$ required for the channel to remain in an open conformation.

As previously suggested, it is possible that this collapse of current at pH 6.4 may occur through destabilization of the open state by a change in the conformation of the turret which breaks the stabilizing bond between E418 and G452 in *Shaker* channels. Elevation of $K^+_o$ decreases the amount of closed state inactivation by stabilizing the selectivity filter through occupation of the outer $K^+$ binding site, increasing $g_{max}$, and thus increasing the macroscopic current. Thus, with a high $K^+_o$, a smaller proportion of the channels will undergo a closed state inactivation process (conductance collapse) and consequently $g_{max}$ (and therefore $I_{max}$) will be larger.

At pH 7.4, Kv1.5 H463R/R487H has recordable outward currents with a $K^+_o$ of 0 mM, 3.5 mM, 10 mM and 140 mM (Figure 6C). At this pH the maximal current (but not necessarily *gmax*) occurs at 10 mM $K^+_o$, despite the lower driving force when compared

to both 0 mM and 3.5 mM $K^+_o$. This result suggests that at pH 7.4, while there is a reduced amount of closed state inactivation, some of the channels have a destabilized open conformation at rest and will rapidly inactivate with depolarization (Lopez-Barneo *et al.*, 1993; Kehl *et al.*, 2002).

At pH 8.4, the $K^+_o$ dependence of $I_{max}$ appears to be the same as pH 7.4 (Figure 5E). The maximal current with 10 mM $K^+_o$ indicates that there is still a high proportion of closed state inactivation in the double mutant with 0 mM and 3.5 mM $K^+_o$. While it has been speculated in the previous 3 paragraphs that the reduction of $g_{max}$ is occurring through a closed state inactivation process, it is possible that another mechanism is causing the observed changes seen in the $I_{max}$ and $K_D$. The rightward shift of the $K_D$, in comparison to wild-type Kv1.5 (greater than 1 mM), may indicate that in Kv1.5 H463R/R487H there is a change in the structure of the pore (possibly a change in the shape of the outer vestibule) that requires a higher concentration of $K^+_o$ to stabilize the open conformation. The changes in $I_{max}$ and $K_D$ may be occurring through a mechanism distinct from a closed-state inactivation process, however, it is indistinguishable from the experiments in this section.

In Kv1.5 H463Q/R487H, neutralization of the charge at 463 restores channel kinetics to wild-type values. At pH 6.4, 0 mM $K^+_o$, there is no collapse of the current (more stable than wild-type) suggesting that neutralization of this residue has stabilized the open conformation and reduced the amount of closed state inactivation. To account for the altered kinetics of Kv1.5 H463R/R487H, I propose that a conformational change occurs in the turret when there is positive charge at position 463 that causes the channel to rapidly inactivate and de-stabilize the open conformation. This hypothesis is supported

as high $K^+_o$ relieves the inactivation seen in the double mutant and neutralization of 463 increases the time constant for inactivation.

In conclusion, the results in this thesis provide further support the concept that there is an interaction between the turret and the pore in Kv1.5. It has been previously reported that altering the charge of R487 (Fedida *et al.*, 1999) and H463 (Jager & Grissmer, 2001; Kehl *et al.*, 2002) can change the rate of inactivation, the $K^+_o$ sensitivity and maximal outward current ($I_{max}$). In this thesis I have shown that a 'permanently' charged residue at position 463 in Kv1.5 accelerates inactivation at pH 6.4, 7.4 and 8.4, and that the rate of inactivation is slowed with 140 mM $K^+_o$ suggesting a link between outer pore inactivation and the turret of Kv1.5.

**Reference List**


Aggarwal, S. K. & Mackinnon, R. (1996). Contribution of the S4 segment to gating charge in the Shaker K+ channel. *Neuron* **16**, 1169-1177.

Aldrich, R. W., Hoshi, T., & Zagotta, W. N. (1990). Differences in gating among amino-terminal variants of Shaker potassium channels. *Cold Spring Harb.Symp.Quant.Biol.* **55**, 19-27.

Almers, W. & McCleskey, E. W. (1984). Non-selective conductance in calcium channels of frog muscle: calcium selectivity in a single-file pore. *J.Physiol* **353**, 585-608.

Begenisich, T. B. & Cahalan, M. D. (1980a). Sodium channel permeation in squid axons. I: Reversal potential experiments. *J.Physiol* **307**, 217-242.

Begenisich, T. B. & Cahalan, M. D. (1980b). Sodium channel permeation in squid axons. II: Non-independence and current-voltage relations. *J.Physiol* **307**, 243-257.

Bezanilla, F., Perozo, E., Papazian, D. M., & Stefani, E. (1991). Molecular basis of gating charge immobilization in Shaker potassium channels. *Science* **254**, 679-683.

Brelidze, T. I., Niu, X., & Magleby, K. L. (2003). A ring of eight conserved negatively charged amino acids doubles the conductance of BK channels and prevents inward rectification. *Proc.Natl.Acad.Sci.U.S.A* **100**, 9017-9022.

Consiglio, J. F., Andalib, P., & Korn, S. J. (2003). Influence of pore residues on permeation properties in the Kv2.1 potassium channel. Evidence for a selective functional interaction of K+ with the outer vestibule. *J.Gen.Physiol* **121**, 111-124.

De Biasi, M., Hartmann, H. A., Drewe, J. A., Taglialatela, M., Brown, A. M., & Kirsch, G. E. (1993). Inactivation determined by a single site in $K^+$ pores. *Pflugers Arch.* **422**, 354-363.

Demo, S. D. & Yellen, G. (1992). Ion effects on gating of the Ca(2+)-activated K+ channel correlate with occupancy of the pore. *Biophys.J.* **61**, 639-648.

Doyle, D. A., Morais, C. J., Pfuetzner, R. A., Kuo, A., Gulbis, J. M., Cohen, S. L., Chait, B. T., & Mackinnon, R. (1998). The structure of the potassium channel: molecular basis of K+ conduction and selectivity. *Science* **280**, 69-77.

Eduljee, C., Chiang , D., Fedida, D., & Kehl, S. J. Inactivation and external potassium-dependence of the hKv1.5 channel can be modulated by altering the biophysical properties of the turret residue at position 463. Biophys.J. 86, 534A. 2004.
Ref Type: Abstract

Elinder, F., Madeja, M., & Arhem, P. (1996). Surface Charges of K channels. Effects of strontium on five cloned channels expressed in Xenopus oocytes. *J.Gen.Physiol* **108**, 325-332.

Elinder, F., Mannikko, R., & Larsson, H. P. (2001). S4 charges move close to residues in the pore domain during activation in a K channel. *J.Gen.Physiol* **118**, 1-10.

Fedida, D., Maruoka, N. D., & Lin, S. (1999). Modulation of slow inactivation in human cardiac Kv1.5 channels by extra- and intracellular permeant cations. *J.Physiol* **515 ( Pt 2)**, 315-329.

Fedida, D., Wible, B., Wang, Z., Fermini, B., Faust, F., Nattel, S., & Brown, A. M. (1993). Identity of a novel delayed rectifier current from human heart with a cloned $K^+$ channel current. *Circ.Res.* **73**, 210-216.

Gandhi, C. S., Clark, E., Loots, E., Pralle, A., & Isacoff, E. Y. (2003). The orientation and molecular movement of a $K^+$ channel voltage-sensing domain. *Neuron* **40**, 515-525.

Gandhi, C. S., Loots, E., & Isacoff, E. Y. (2000). Reconstructing voltage sensor-pore interaction from a fluorescence scan of a voltage-gated K+ channel. *Neuron* **27**, 585-595.

Grissmer, S. & Cahalan, M. (1989). TEA prevents inactivation while blocking open $K^+$ channels in human T lymphocytes. *Biophys.J.* **55**, 203-206.

Haug, T., Sigg, D., Ciani, S., Toro, L., Stefani, E., & Olcese, R. (2004). Regulation of K+ flow by a ring of negative charges in the outer pore of BKCa channels. Part I: Aspartate 292 modulates K+ conduction by external surface charge effect. *J.Gen.Physiol* **124**, 173-184.

Heginbotham, L., Lu, Z., Abramson, T., & Mackinnon, R. (1994). Mutations in the $K^+$ channel signature sequence. *Biophys.J.* **66**, 1061-1067.

Hess, P. & Tsien, R. W. (1984). Mechanism of ion permeation through calcium channels. *Nature* **309**, 453-456.

Hille B (2001). *Ion Channels of Excitable Membranes* Sinauer Associates, Sunderland, MA.

Hodgkin, A. L. & Huxley, A. F. (1952a). A quantitative description of membrane current and its application to conduction and excitation in nerve. *J.Physiol* **117**, 500-544.

Hodgkin, A. L. & Huxley, A. F. (1952b). Currents carried by sodium and potassium ions through the membrane of the giant axon of Loligo. *J.Physiol* **116**, 449-472.

Hodgkin, A. L., Huxley, A. F., & KATZ, B. (1952). Measurement of current-voltage relations in the membrane of the giant axon of Loligo. *J.Physiol* **116**, 424-448.

Hoshi, T., Zagotta, W. N., & Aldrich, R. W. (1990). Biophysical and molecular mechanisms of Shaker potassium channel inactivation. *Science* **250**, 533-538.

Hoshi, T., Zagotta, W. N., & Aldrich, R. W. (1991). Two types of inactivation in Shaker $K^+$ channels: effects of alterations in the carboxy-terminal region. *Neuron* **7**, 547-556.

Hoshi, T., Zagotta, W. N., & Aldrich, R. W. (1994). Shaker potassium channel gating. I: Transitions near the open state. *J.Gen.Physiol* **103**, 249-278.

Imoto, K., Busch, C., Sakmann, B., Mishina, M., Konno, T., Nakai, J., Bujo, H., Mori, Y., Fukuda, K., & Numa, S. (1988). Rings of negatively charged amino acids determine the acetylcholine receptor channel conductance. *Nature* **335**, 645-648.

Jager, H. & Grissmer, S. (2001). Regulation of a mammalian Shaker-related potassium channel, hKv1.5, by extracellular potassium and pH. *FEBS Lett.* **488**, 45-50.

Jager, H., Rauer, H., Nguyen, A. N., Aiyar, J., Chandy, K. G., & Grissmer, S. (1998). Regulation of mammalian Shaker-related $K^+$ channels: evidence for non-conducting closed and non-conducting inactivated states. *J.Physiol* **506 ( Pt 2)**, 291-301.

Jiang, Y., Lee, A., Chen, J., Cadene, M., Chait, B. T., & Mackinnon, R. (2002). The open pore conformation of potassium channels. *Nature* **417**, 523-526.

Jiang, Y., Lee, A., Chen, J., Ruta, V., Cadene, M., Chait, B. T., & Mackinnon, R. (2003a). X-ray structure of a voltage-dependent $K^+$ channel. *Nature* **423**, 33-41.

Jiang, Y., Ruta, V., Chen, J., Lee, A., & Mackinnon, R. (2003b). The principle of gating charge movement in a voltage-dependent $K^+$ channel. *Nature* **423**, 42-48.

Kamb, A., Tseng-Crank, J., & Tanouye, M. A. (1988). Multiple products of the Drosophila Shaker gene may contribute to potassium channel diversity. *Neuron* **1**, 421-430.

Kehl, S. J., Eduljee, C., Kwan, D. C., Zhang, S., & Fedida, D. (2002). Molecular determinants of the inhibition of human Kv1.5 potassium currents by external protons and $Zn^{2+}$. *J.Physiol* **541**, 9-24.

Kwan, D. C., Eduljee, C., Lee, L., Zhang, S., Fedida, D., & Kehl, S. J. (2004a). The external K+ concentration and mutations in the outer pore mouth affect the inhibition of kv1.5 current by $Ni^{2+}$. *Biophys.J.* **86**, 2238-2250.

Kwan, D. C., Zhang, S., Fedida, D., & Kehl, S. J. Induction of voltage-dependent decay in hKv1.5 by intracellular $Ca^{2+}{}_i$ or $Mg^{2+}{}_i$. Biophys.J. 86, 534A. 2004b. Ref Type: Abstract

Laine, M., Lin, M. C., Bannister, J. P., Silverman, W. R., Mock, A. F., Roux, B., & Papazian, D. M. (2003). Atomic proximity between S4 segment and pore domain in Shaker potassium channels. *Neuron* **39**, 467-481.

Larsson, H. P., Baker, O. S., Dhillon, D. S., & Isacoff, E. Y. (1996). Transmembrane movement of the shaker $K^+$ channel S4. *Neuron* **16**, 387-397.

Larsson, H. P. & Elinder, F. (2000). A conserved glutamate is important for slow inactivation in $K^+$ channels. *Neuron* **27**, 573-583.

Latorre, R. (1989). Ion channel modulation by divalent cations. *Acta Physiol Scand.Suppl* **582**, 13.

Latorre, R., Oberhauser, A., Labarca, P., & Alvarez, O. (1989). Varieties of calcium-activated potassium channels. *Annu.Rev.Physiol* **51**, 385-399.

Li, R. A., Velez, P., Chiamvimonvat, N., Tomaselli, G. F., & Marban, E. (2000). Charged residues between the selectivity filter and S6 segments contribute to the permeation phenotype of the sodium channel. *J.Gen.Physiol* **115**, 81-92.

Liman, E. R., Hess, P., Weaver, F., & Koren, G. (1991). Voltage-sensing residues in the S4 region of a mammalian $K^+$ channel. *Nature* **353**, 752-756.

Liu, Y., Jurman, M. E., & Yellen, G. (1996). Dynamic rearrangement of the outer mouth of a $K^+$ channel during gating. *Neuron* **16**, 859-867.

Logothetis, D. E., Kammen, B. F., Lindpaintner, K., Bisbas, D., & Nadal-Ginard, B. (1993). Gating charge differences between two voltage-gated $K^+$ channels are due to the specific charge content of their respective S4 regions. *Neuron* **10**, 1121-1129.

Logothetis, D. E., Movahedi, S., Satler, C., Lindpaintner, K., & Nadal-Ginard, B. (1992). Incremental reductions of positive charge within the S4 region of a voltage-gated $K^+$ channel result in corresponding decreases in gating charge. *Neuron* **8**, 531-540.

Long, S. B., Campbell, E. B., & Mackinnon, R. (2005). Voltage Sensor of Kv1.2: Structural Basis of Electromechanical Coupling. *Science.*

Loots, E. & Isacoff, E. Y. (1998). Protein rearrangements underlying slow inactivation of the Shaker $K^+$ channel. *J.Gen.Physiol* **112**, 377-389.

Lopez-Barneo, J., Hoshi, T., Heinemann, S. H., & Aldrich, R. W. (1993). Effects of external cations and mutations in the pore region on C-type inactivation of Shaker potassium channels. *Receptors.Channels* **1**, 61-71.

Ludewig, U., Lorra, C., Pongs, O., & Heinemann, S. H. (1993). A site accessible to extracellular $TEA^+$ and $K^+$ influences intracellular $Mg^{2+}$ block of cloned potassium channels. *Eur.Biophys.J.* **22**, 237-247.

Mackinnon, R. (1991a). Determination of the subunit stoichiometry of a voltage-activated potassium channel. *Nature* **350**, 232-235.

Mackinnon, R. (1991b). New insights into the structure and function of potassium channels. *Curr.Opin.Neurobiol.* **1**, 14-19.

Mackinnon, R. (2003). Potassium channels. *FEBS Lett.* **555**, 62-65.

Mackinnon, R., Aldrich, R. W., & Lee, A. W. (1993). Functional stoichiometry of Shaker potassium channel inactivation. *Science* **262**, 757-759.

Mackinnon, R., Latorre, R., & Miller, C. (1989). Role of surface electrostatics in the operation of a high-conductance $Ca^{2+}$-activated $K^+$ channel. *Biochemistry* **28**, 8092-8099.

Mackinnon, R. & Yellen, G. (1990). Mutations affecting TEA blockade and ion permeation in voltage-activated $K^+$ channels. *Science* **250**, 276-279.

Matsuda, H., Saigusa, A., & Irisawa, H. (1987). Ohmic conductance through the inwardly rectifying K channel and blocking by internal $Mg^{2+}$. *Nature* **325**, 156-159.

Matteson, D. R. & Swenson, R. P. (1986). External monovalent cations that impede the closing of K channels. *J.Gen.Physiol* **87**, 795-816.

Molina, A., Ortega-Saenz, P., & Lopez-Barneo, J. (1998). Pore mutations alter closing and opening kinetics in Shaker $K^+$ channels. *J.Physiol* **509 ( Pt 2)**, 327-337.

Nimigean, C. M., Chappie, J. S., & Miller, C. (2003). Electrostatic tuning of ion conductance in potassium channels. *Biochemistry* **42**, 9263-9268.

Ortega-Saenz, P., Pardal, R., Castellano, A., & Lopez-Barneo, J. (2000). Collapse of conductance is prevented by a glutamate residue conserved in voltage-dependent $K^+$ channels. *J.Gen.Physiol* **116**, 181-190.

Papazian, D. M., Timpe, L. C., Jan, Y. N., & Jan, L. Y. (1991). Alteration of voltage-dependence of Shaker potassium channel by mutations in the S4 sequence. *Nature* **349**, 305-310.

Pardo, L. A., Heinemann, S. H., Terlau, H., Ludewig, U., Lorra, C., Pongs, O., & Stuhmer, W. (1992). Extracellular $K^+$ specifically modulates a rat brain $K^+$ channel. *Proc.Natl.Acad.Sci.U.S.A* **89**, 2466-2470.

Perez-Cornejo, P. (1999). $H^+$ ion modulation of C-type inactivation of Shaker $K^+$ channels. *Pflugers Arch.* **437**, 865-870.

Perez-Cornejo, P., Stampe, P., & Begenisich, T. (1998). Proton probing of the charybdotoxin binding site of Shaker $K^+$ channels. *J.Gen.Physiol* **111**, 441-450.

Perozo, E., Santacruz-Toloza, L., Stefani, E., Bezanilla, F., & Papazian, D. M. (1994). S4 mutations alter gating currents of Shaker K channels. *Biophys.J.* **66**, 345-354.

Seoh, S. A., Sigg, D., Papazian, D. M., & Bezanilla, F. (1996). Voltage-sensing residues in the S2 and S4 segments of the Shaker K+ channel. *Neuron* **16**, 1159-1167.

Sigg, D., Stefani, E., & Bezanilla, F. (1994). Gating current noise produced by elementary transitions in Shaker potassium channels. *Science* **264**, 578-582.

Smith-Maxwell, C. J., Ledwell, J. L., & Aldrich, R. W. (1998). Role of the S4 in cooperativity of voltage-dependent potassium channel activation. *J.Gen.Physiol* **111**, 399-420.

Smith, P. L., Baukrowitz, T., & Yellen, G. (1996). The inward rectification mechanism of the HERG cardiac potassium channel. *Nature* **379**, 833-836.

Smith, S. S., Liu, X., Zhang, Z. R., Sun, F., Kriewall, T. E., McCarty, N. A., & Dawson, D. C. (2001). CFTR: covalent and noncovalent modification suggests a role for fixed charges in anion conduction. *J.Gen.Physiol* **118**, 407-431.

Steidl, J. V. & Yool, A. J. (1999). Differential sensitivity of voltage-gated potassium channels Kv1.5 and Kv1.2 to acidic pH and molecular identification of pH sensor. *Mol.Pharmacol.* **55**, 812-820.

Swenson, R. P. & Armstrong, C. M. (1981). $K^+$ channels close more slowly in the presence of external $K^+$ and $Rb^+$. *Nature* **291**, 427-429.

Tempel, B. L., Papazian, D. M., Schwarz, T. L., Jan, Y. N., & Jan, L. Y. (1987). Sequence of a probable potassium channel component encoded at Shaker locus of Drosophila. *Science* **237**, 770-775.

Trapani, J. G. & Korn, S. J. (2003). Effect of external pH on activation of the Kv1.5 potassium channel. *Biophys.J.* **84**, 195-204.

Wang, S., Bondarenko, V. E., Qu, Y., Morales, M. J., Rasmusson, R. L., & Strauss, H. C. (2004). Activation properties of Kv4.3 channels: time, voltage and $K^+o$ dependence. *J.Physiol* **557**, 705-717.

Wang, S., Liu, S., Morales, M. J., Strauss, H. C., & Rasmusson, R. L. (1997). A quantitative analysis of the activation and inactivation kinetics of HERG expressed in Xenopus oocytes. *J.Physiol* **502 ( Pt 1)**, 45-60.

Yang, N., George, A. L., Jr., & Horn, R. (1996). Molecular basis of charge movement in voltage-gated sodium channels. *Neuron* **16**, 113-122.

Yellen, G., Jurman, M. E., Abramson, T., & Mackinnon, R. (1991). Mutations affecting internal TEA blockade identify the probable pore-forming region of a $K^+$ channel. *Science* **251**, 939-942.

Yellen, G., Sodickson, D., Chen, T. Y., & Jurman, M. E. (1994). An engineered cysteine in the external mouth of a $K^+$ channel allows inactivation to be modulated by metal binding. *Biophys.J.* **66**, 1068-1075.

Zagotta, W. N., Hoshi, T., & Aldrich, R. W. (1990b). Restoration of inactivation in mutants of Shaker potassium channels by a peptide derived from ShB. *Science* **250**, 568-571.

Zagotta, W. N., Hoshi, T., & Aldrich, R. W. (1990a). Restoration of inactivation in mutants of Shaker potassium channels by a peptide derived from ShB. *Science* **250**, 568-571.

Zagotta, W. N., Hoshi, T., & Aldrich, R. W. (1994a). Shaker potassium channel gating. III: Evaluation of kinetic models for activation. *J.Gen.Physiol* **103**, 321-362.

Zagotta, W. N., Hoshi, T., Dittman, J., & Aldrich, R. W. (1994b). Shaker potassium channel gating. II: Transitions in the activation pathway. *J.Gen.Physiol* **103**, 279-319.

Zhou, Y., Morais-Cabral, J. H., Kaufman, A., & Mackinnon, R. (2001). Chemistry of ion coordination and hydration revealed by a $K^+$ channel-Fab complex at 2.0 A resolution. *Nature* **414**, 43-48.

## Appendix I- hERG Experiments

### Molecular Determinants of Inactivation in hERG Potassium Channels

The human ether-a-go-go (eag) gene was originally identified in *Drosophilla* as a result of a leg shaking phenotype from an increase in neuronal excitability (Ganetzky & Wu, 1983). Expression of the eag polypeptide in frog oocytes confirmed that the eag gene does encode for a potassium channel (Bruggemann *et al.*, 1993).

The human eag polypeptide hERG (human ether a-go-go related gene) was originally isolated from human hippocampal tissue and encodes for an inwardly rectifying potassium channel (Warmke & Ganetzky, 1994).

### Structure of the hERG channel

The hERG channel has a similar molecular composition to that of most voltage gated ion channels. Potassium channels are tetrameric assemblies, that contain 6 transmembrane (TM) regions in each domain (Hille 2001). The P-loop in hERG channels is different from that of most voltage gated $K^+$ channels as it is comprised of 39 amino acids, whereas, most other channels have ~10-12 amino acids in their p-loops.

### Channel Kinetics

In the heart, hERG channels play an important role in cardiac repolarization. These channels are partly responsible for the delayed rectifier $K^+$ current ($I_{kr}$), a current that is responsible for returning the cell to it's resting membrane potential (~-70mV) (Sanguinetti & Jurkiewicz, 1990; Sanguinetti *et al.*, 1995). hERG potassium channels are unusual in that the rate constant for channel activation is slower than that of channel inactivation. With depolarization, hERG channels slowly activate but are rapidly inactivated as the membrane voltage reaches more positive potentials. As the cardiac action potential repolarizes channel inactivation is rapidly removed, generating a large

outward potassium current that quickly returns the cell to resting membrane potential. Reduction of this current, by mutation or blockade, has been shown to cause some types of long-QT syndrome (Zhang *et al.*, 2001).

**Inactivation**

Unlike C-type inactivation in Shaker potassium channels, the inactivation process in hERG appears to possess intrinsic voltage dependence (Smith *et al.*, 1996). Although the molecular mechanisms for hERG inactivation are not completely understood, it has proposed that hERG channels may possess a voltage sensor that regulates the rate of inactivation (Johnson, Jr. *et al.*, 1999; Zhang *et al.*, 2004).

**Divalent Cations Modulate Channel Activity**

In hERG channels extracellular divalent cations ($Mg^{2+}$, $Ca^{2+}$ and $Zn^{2+}$) reduce the magnitude of outward currents, whereas, $Na^{+}_{o}$ blocks outward currents through hERG Channels. In contrast to the effects of the afore mentioned cations, $Cd^{2+}_{o}$ increases the magnitude of outward currents by destabilizing the inactivated state of hERG. This destabilization of the inactivated state allows the hERG channel to have larger current magnitude in both the pre-pulse (+50mV) and the repolarizing pulse (-40mV).

**Hypothesis**

The aim of this project was to determine the mechanism by which $Cd^{2+}_{o}$ acts on hERG channels to cause this paradoxical increase in current magnitude. It has previously been shown that $Cd^{2+}$ ions have a high affinity for cysteine and histidine residues. In the turret region of hERG channels there are 2 histidine residues (H578 and H587) that have been postulated, through a loop-turn-helix structure, to come in close atomic proximity during channel activation. Mutation of these residues has a profound effect on channel kinetics,

significantly altering the rate of inactivation. The goal of this project was to determine the binding site for $Cd^{2+}$ ions in hERG and the role of H578 and H587 in channel kinetics.

**Methods**

The hERG channel nucleotide sequence has a high proportion (~55%) of the nucleotide bases guanosine (G) Cytosine (C) and as a result significant internal homology. In Site-Directed Mutagenesis, a mutant (containing the desired mutation) primer binds to a region of the nucleotide sequence with which it shares a high degree of homology. Because of the internal homology in hERG, it is extremely difficult to create a primer that is specific to one region of the channel. Non-specific primer binding is a very common occurrence. When this occurs it creates mutations at incorrect positions, or more than likely no mutation is created because the primer is binding in so many positions. The following methods section will explain some of the procedures and cloning strategies that I used to create 6 hERG channel mutants (H578C, H587C, H578C/H587C, H578Q, H587Q and H578Q/H587Q).

**Site-Directed Mutagenesis**

Initially, I attempted to create the mutants using the most common, and convenient, approach to generate a mutation at a specific site.

Reaction Mixture
50ng Template
1X Rxn Buffer (PFU Turbo)
125 ng up primer
125 ng dn primer
0.2mM dNTP's
$dH_20$- volume to 49.5µl
0.5µl of PFU Turbo DNA Polymerase

In this protocol, the dsDNA sequence is first heated to 95°C to separate the complimentary DNA strands. In the second, the reaction mixture is cooled to a

temperature near the melting point of the mutant primers (~55-60°C), at which they will bind to a region of the ssDNA that shares high homology. The mixture is then heated to 72°C for 6min (1min/1kB) and then the process is repeated 30x. If the protocol is successful, the hERG sequence that has incorporated the mutant will be amplified and sequencing will confirm the presence of a mutant channel. This approach was unsuccessful in generating hERG mutants.

The following modifications were made in an attempt to generate the correct hERG mutants.

*25-200ng template*: It has previously been reported that decreasing the concentration of the template can decrease the probability of non-specific primer binding; whereas, increasing the concentration of the template would increase the probability that the primer would bind to the sequence (however, not necessarily at the proper site) and generate a mutated channel. Altering the concentration of template was found to have no effect on the efficiency of the QuikChange mutagenesis kit.

*1x Buffer*: Not altered

*125ng up primer*: The amount of primer was increased in an attempt to increase the probability that the primer would bind at the correct location. This was also shown to have no effect on the efficiency of the reaction.

*125ng dn primer*: Same as the up primer.

*0.2mM dNTPs*: 0.2mM is a more than sufficient concentration of nucleotide bases, and the recommended amount, for the QuikChange Mutagenesis kit, thus it was not altered.

**Alterations to the Protocol:**

*Betaine*

It was found that addition of 1.3M Betaine increased the probability that the primers would bind at the correct location. Betaine acts to decrease the probability that during the cooling process (95°C to 55°C) that the highly homologous hERG sequence will not just re-anneal before the primers are able to bind at the correct location(Henke *et al.*, 1997).

*Cooling Temperature*

In attempt to increase the efficiency at which the primer was able to bind to hERG a cooling temperature between 55° and 62°C was used.

*DNA Polymerase*

In addition to PFU Turbo, VENT Polymerase and KOD Hot Start Polymerase enzymes were added to the reaction mixture. It was found that these enzymes did not alter the efficiency of the mutagenesis.

*Succesful Protocol*

Using the QuikChange kit, the hERG H578C mutant was created. The successful reaction mixture is listed below. This exact recipe did not generate any of the other mutants.

50ng template
1x Buffer
125ng up primer
125ng dn primer
0.2mM dNTPs
1.3M Betaine
$dH_2O$- volume to 49.5μl
0.5μl PFU Turbo DNA Polymerase

PCR
Step 1: 95°C for 45s
Step 2: 56°C for 45s
Step 3: 72°C for 5min
Repeat 1-3 29x
Step 4: 72°C for 15min
End

**Vector**

The pcDNA3 vector is ~3.5kB and it contains a relatively equal proportion of G, C, A and T nucleotide bases. However, there are 2 regions in the sequence that contain sequences that are rich in GC bases. In an attempt to decrease the probability that the mutant primers may be binding to a nucleotide sequence in the pcDNA3 vector, I removed hERG from pcDNA3 using the restriction enzymes EcoRI and HindIII and subcloned it into pUC19. pUC19 is a small vector (2.7kB) that still confers ampicillin resistance; however, it lacks the GC rich regions that are present in pcDNA3. Using the above reaction mixture I was unable to create any of the other mutants.

**Subsequent Mutagenesis Methods**

The previous result suggested to me that the vector was not the reason that the QuikChange mutagenesis kit was not working in the hERG channel. In an attempt to decrease inadvertent binding during the QuikChange mutagenesis I subcloned a smaller fragment of hERG using ClaI and SbfI (~1.1kB) into pcDNA3 and attempted the QuikChange mutagenesis protocol. Unfortunately, I was still unable to create the desired mutants using this smaller form of the channel in pcDNA3.

**2-Step PCR**

Prior to the development of Site-Directed Mutagenesis and mutagenesis kits mutations at specific sites were engineered using a 2-step PCR protocol. In this protocol the following reaction mixture can be used to generate a specific mutation:

5ng DNA template
3mM $MgS0_4$
1x Buffer
0.1mM dNTPs

25pmol hERG oligo primer (up or dn)
25pmol hERG Mutant primer (dn or up)
1.3M Betaine
$dH_20$- Volume to 49.5µl
0.5µl DNA Polymerase

In this protocol, similar to Quikchange site-directed mutagenesis, the reaction mixture is heated to 95°C, cooled to 58°C, and then heated to 72°C to allow amplification of the templates by the DNA polymerase. As the templates are cooled from 95°C to 58°C, the mutant primer and oligo primer bind at their consensus sequence sites. As the mixture is heated to 72°C the oligo primer (no mutation) is extended and amplifies the DNA up to the location of the mutant primer. After the primer the polymerase is unable to extend the sequence any further. This procedure results in large mutant fragments (up and dn) being generated. Thus, rather than using a primer that consists of only 25bp one is able to use a primer product of ~500bp that should bind at only region of the channel, increasing the efficiency of the mutagenesis.

Once both of the large mutant products have been made, here is the reaction mixture.

2ng Up Fragment
2ng Dn Fragment
3mM $MgSO_4$
1x Buffer
0.1mM dNTPs
25pmol Up Primer (Herg Up)
25pmol Dn primer (New Herg Dn)
1.3M Betaine
$dH_2O$ Volume to 49.5µl
0.5µl DNA Polymerase

If this procedure is successful it will generate a mutant fragment that is the size of the distance between the Up and Dn (non-mutant) primers. In this instance it generated a fragment that was 1.1kB in length, as expected. The fragment was then cut using the restriction enzymes BstEII and SbfI and ligated back into full length hERG in a pcDNA3

vector. Using this method all of the other mutations were created. Double mutants (H578C/H587C and H578Q/H587Q) were made using the 2-step PCR method; however, the template contained had a previously engineered mutation at 578 or 587 to either a C or Q.

*Effect of $MgSO_4$ on 2-Step PCR*

$MgSO_4$, a compound found in the enzyme buffer, was found to have a significant effect on the efficiency of the PCR. In all of the PCR reactions 2mM, 3mM, and 4mM $MgSO_4$ was added to the mixture. There was no discernable trend, however, different hERG mutants were generated by different $MgS0_4$ concentrations. The hERG mutants were generated using all 3 concentrations of $MgS0_4$.

*Primer Binding Temperature*

The effect of temperature in the second step, as with the QuikChange kit was very specific to the primer that was being used in the reaction, even though all of the primers had approximately the same $A_T$.

Here is a table showing the optimal [$MgSO_4$] and $A_T$

H578C: QuikChange Kit
H587C: 3 or 4mM $MgSO_4$, $A_T$= 55°C
H578C/H587C: see above results
H578Q: 2mM $MgSO_4$ $A_T$= 57°C
H587Q: 3 or 4mM $MgSO_4$, $A_T$ = 60°C and 59°C respectively
H578Q/H587Q: see above results

**Electrophysiological Recordings**

A common difficulty in working with wild-type hERG is the low expression rate that it shows in all mammalian cell lines. An HEK cell line was used for all of the recordings done on wild-type hERG channels and H578C. In a stably expressing HEK cell line the

average amplitude of tail currents at –40mV was ~1.5nA. In general, stably expressing cell lines express the channel of interest with a higher efficiency than a transfected cell with the same channel. The fact that hERG is expressed so poorly made recording from mutant channels extremely difficult as there was, in ~80% of the cells, no expression. This difficulty is overcome in many labs through the use of *Xenoups laevis* oocyte's. The larger size, cooler intracellular temperature and increased efficiency of the transcription and translation machinery allows these cells to express hERG at levels in which μA currents can be recorded. The problem with this approach, and this was very evident at the recent biophysical conference (Long Beach California, CA, USA) is the difficulty of obtaining accurate voltage-control of the cell. In oocytes the enhancement of hERG currents by $Cd^{2+}$ was not evident in an oocyte system; whereas, in mammalian cells expressing hERG, the current is enhanced. The only preliminary data that was obtained from the H578C mutant indicated that a cysteine at position 578, and not a histidine, may disrupt the $Cd^{2+}$ binding site formed by the histidines at 578 and 587. Disruption of this site reduced the affinity of $Cd^{2+}$ for this site and ablated its effect on hERG channels.

**Reference List**


Bruggemann, A., Pardo, L. A., Stuhmer, W., & Pongs, O. (1993). Ether-a-go-go encodes a voltage-gated channel permeable to K+ and Ca2+ and modulated by cAMP. *Nature* **365**, 445-448.

Ganetzky, B. & Wu, C. F. (1983). Neurogenetic analysis of potassium currents in Drosophila: synergistic effects on neuromuscular transmission in double mutants. *J.Neurogenet.* **1**, 17-28.

Henke, W., Herdel, K., Jung, K., Schnorr, D., & Loening, S. A. (1997). Betaine improves the PCR amplification of GC-rich DNA sequences. *Nucleic Acids Res.* **25**, 3957-3958.

Johnson, J. P., Jr., Balser, J. R., & Bennett, P. B. (1999). Enhancement of HERG K(+) currents by Cd(2+) destabilization of the inactivated state. *Biophys.J.* **77**, 2534-2541.

Sanguinetti, M. C., Jiang, C., Curran, M. E., & Keating, M. T. (1995). A mechanistic link between an inherited and an acquired cardiac arrhythmia: HERG encodes the IKr potassium channel. *Cell* **81**, 299-307.

Sanguinetti, M. C. & Jurkiewicz, N. K. (1990). Two components of cardiac delayed rectifier K+ current. Differential sensitivity to block by class III antiarrhythmic agents. *J.Gen.Physiol* **96**, 195-215.

Smith, P. L., Baukrowitz, T., & Yellen, G. (1996). The inward rectification mechanism of the HERG cardiac potassium channel. *Nature* **379**, 833-836.

Warmke, J. W. & Ganetzky, B. (1994). A family of potassium channel genes related to eag in Drosophila and mammals. *Proc.Natl.Acad.Sci.U.S.A* **91**, 3438-3442.

Zhang, M., Liu, J., & Tseng, G. N. (2004). Gating charges in the activation and inactivation processes of the HERG channel. *J.Gen.Physiol* **124**, 703-718.

Zhang, S., Rajamani, S., Chen, Y., Gong, Q., Rong, Y., Zhou, Z., Ruoho, A., & January, C. T. (2001). Cocaine blocks HERG, but not KvLQT1+minK, potassium channels. *Mol.Pharmacol.* **59**, 1069-1076.

Appendix II- Code for Eyring-Rate Model

```
#pragma rtGlobals=0
Function Gamma1()

make/o/n=(4,4) k=0          //make/overwrite a 4x4 matrix k in which to put the rate
constants
make /o/n=(200) Vm
make/o/n=(200) flux_of_A
make/o/n=(200) net_flux
make/o/n=(200) Current

variable/g a_o, a_i          // the ion concentrations inside and outside
variable/g p1a, p2a, p3a, s1a,s2a      // parameters for the energy profile in RT units for
ion A
variable/g d1, d2, d3        // the electrical distance between peaks and wells
variable/g TC, TK                  // the temperature in Celsius and Kelvin
variable R = 8.314472        // the gas constant in J mole-1 K-1 (= V C mole-1 K-1)
variable F = 96485.3415      // the Faraday constant in C mole-1
variable/g fort
variable ff                        // the frequency factor which is kT/h
variable kb = 1.38e-23             // Boltzmann's constant in J K-1
variable hc = 6.62606891e-34       // Planck's constant in J s
variable V
variable/g summ
variable i,j,index
variable P1, k12, P2, k21

// set internal and external concentrations of ion A

a_o = 0.14          // the external concentration of ion A in molar
a_i = 0.14          // the internal concentration of ion A in molar

// set energy peaks and wells for ion A

p1a = 5                    //in Rt units
p2a = -6
p3a = 5
s1a = -10
s2a = -9

// set electrical distances between energy minima and maxima

d1 =1/6
d2 = 1/6
d3 =1/6
```

```
// set temperature

TC = 20
TK = 273+ TC
fort = F/(R*TK)                    // where fort is F over RT (F/RT)
ff = kb * TK  / hc                 // gives a frequency of vibration of ca. 6e12 s-1

index=0

for (V = -100; V < 100; V += 1)

i=0
do
        j=0
                do
                        k[i][j] = 0                    //initialize matrix to 0
                        j += 1
                while (j < 4)
        i += 1
while (i < 4)

// set up matrix k with rate constant values

// rate constants for A

// A entering/leaving outside side (s1a)

k[0][1] = a_o * ff * exp(-(p1a + d1 * V/1000 * fort))          // k01 (EC to
outside site)
k[1][0] = ff * exp(-(p1a - s1a - d1 * V/1000 * fort))          // k10 (outside site to
EC)

k[2][3] = a_o * ff * exp(-(p1a + d1 * V/1000 * fort))          // k23
(EC to outside site- both occupied)
k[3][2] = ff * exp(-(p1a - s1a - d1 * V/1000 * fort))          // k32 (outside site to
EC- both occupied)

// A hopping central barrier

k[1][2] = ff * exp(-(p2a - s1a + d1* V/1000 * fort))           // k12 (Inside
to outside site)
k[2][1] = ff * exp(-(p2a - s2a - d1 * V/1000 * fort))          // k21 (Outisde
to inside site)
```

```
// A entering/leaving inside site (s2a)

k[0][2] = a_i * ff * exp(-(p3a - d1 * V/1000 * fort))                    // k02 (IC to
inside site)
k[2][0] = ff * exp(-(p3a - s2a + d1* V/1000 * fort))                     // k20 (Inside site to
IC)

k[1][3] = a_i * ff * exp(-(p3a - d1 * V/1000 * fort))                    // k13 (IC to
inside site- both occupied)
k[3][1] = ff * exp(-(p3a - s2a + d1 * V/1000 * fort))                    // k31 (Inside site to
IC- both occupied)



i=0
j=0
for (i = 0; i < 4; i += 1)
        for (j = 0; j < 4; j +=1)
                if (k[i][j] > 0)
                        k[i][j]/=1e10                                    // divide by 1x10^10 so that
the determinant is within range
                endif
        endfor
endfor


// make diagonal element equal to -sum of non-diagonal elements in the row

i=0
do
        j=0
        summ=0
                do
                        summ+=k[i][j] * (i!=j)          // the element value is not summed if
it is diagonal
                                                        // -- this is not absolutely
necessary
                                                        // since the diagonal elements
should be zero already
                        j+=1
                while (j<4)
        k[i][i] = -summ
        i+=1
while (i<4)
```

```
calc_ss_flux(k)                    //calls the calc_ss_flux routine to calculate the
determinant of the matrix k

// write results of calculation to waves flux_of_A and Vm

P2 = determinant[2][1]
k21 = k[2][1]*1e10

P1 = determinant[1][1]
k12 = k[1][2] *1e10

flux_of_A [index]= P2 * k21-P1*k12
Current[index]=flux_of_A[index]*((1/6.023e23)*F)

Vm[index]=V


index+=1

endfor

End
```

**Calc_ss_flux**

```
#pragma rtGlobals=0

Function calc_ss_flux(input_wavename)
wave input_wavename                    //the matrix containing the rate constants is
passed in the call to the function
string a = "k"
string b
string c
variable j
variable i = dimsize(input_wavename,0)    //get the number of rows in the matrix
//print "matrix dimension is ": i
make/o/n=(i,2) determinant                    //create a [i X 2] matrix in which to
store the determinants (column 1)
                                                                    //and the
probabilities (column 2)
variable dsum = 0          // the sum of the determinants
variable psum=0            // the sum of the probablilities - this is part of a test to see if
the calculation is correct
                                    // i.e., psum should equal 1
```

```
for (j= 0; j<i ; j+=1)
        b=a+"_"+num2str(j)
        //print b
        duplicate/o input_wavename, $b
        deletepoints /M=0 j,1, $b        //delete row i of the duplicated matrix
        deletepoints /M=1 j,1, $b       // delete column i of the duplicated matrix

        determinant[j][0]=matrixdet($b)       // calculate the determinant of the matrix and
store the result
                                                                  // in row j of column 0
        determinant[j][1]=0                   // initialize row j of column 1 to zero
endfor


for (j = 0; j < i ; j += 1)
        dsum+=determinant[j][0]               //get the sum of the values for the
determinants
endfor

for (j = 0 ; j < i ; j += 1)
        determinant[j][1] = determinant[j][0]/dsum  //p = determinant/sum of the
determinants
                                                                                  // store
the result in row j of column 1
endfor



for (j=0 ; j<i ; j+=1)
        psum+=determinant[j][1]                                    //the sum of the
probabilities shoud be 1
endfor

// print "psum = ":psum

end
```